12 July 1965

Final Report

"THEORETICAL STUDY OF THE COUPLING
BETWEEN THE SOLAR WIND AND THE EXOSPHERE"

Prepared for

National Aeronautics and Space Administration
Washington 25, D. C.

Contract No. NASw-698

23 June 1964 to 22 June 1965

Report No. 8

QUANTUM PHYSICS LABORATORY
PHYSICAL RESEARCH DIVISION

TRW SYSTEMS
One Space Park
Redondo Beach, California

National Aeronautics and Space Administration
Contract No. NASw-698

Prepared by _F. L. Scarf_

F. L. Scarf
Theoretical Physics Department

Approved by _S. Altshuler_

S. Altshuler
Manager
Theoretical Physics Department

Approved by _H. C. Corben_

H. C. Corben
Director
Quantum Physics Laboratory

QUANTUM PHYSICS LABORATORY
PHYSICAL RESEARCH DIVISION

TRW SYSTEMS
One Space Park
Redondo Beach, California

Formerly TRW Space Technology Laboratories (STL)

TABLE OF CONTENTS

I. PROGRESS OF WORK (March through June)[*]

The manuscript "Preliminary Report on Detection of Electrostatic Ion Waves in the Magnetosphere" has been accepted for publication in the Journal of Geophysical Research (to appear July 1, 1965) and the Research Note "Direct Detection of Ambient Electron Plasma Oscillation Fields in the Magnetosphere" will appear in J. Planetary and Space Science. The abstract "Large Amplitude Electrostatic Waves above the Ionosphere and Effects on the Plasma Sheath" will not be presented at the AFCRL Symposium (see Status Report No. 7) because the main interest at the Symposium involves lower altitude effects.

During this period Dr. Fredricks attended the Spring American Geophysical Union meeting and delivered the two talks noted in Report No. 7. The manuscripts "Effects of Solar Wind Composition on the Threshold for Plasma Instability in the Transition Region" (Appendix A) and "Production of Superthermal Electrons by Electrostatic Plasma Oscillations" (Appendix B) were completed; the first has been submitted to Journal of Geophysical Research, and a revised version of the second will be submitted to Physics of Fluids.

On April 23, Dr. Scarf and Mr. Crook gave a presentation at NASA Headquarters on the proposal to detect plasma oscillations on OGO E, and work

---

[*] A new contract (NASw-1226) which will extend this work has recently been negotiated and the final report for NASw-698 is also a progress report for continuing research in this area.

has continued on P-11 data reduction. A comprehensive account of these findings is being prepared.

II. KEY PERSONNEL

During this period F. L. Scarf, R. W. Fredricks, S. Altshuler, and A. Peskoff worked on this problem.

III. NEW CONCEPTS

None

IV. SUMMARY OF WORK, NAS w - 698.

Published Articles Generated under NASw-698:

1. A Model for a Broad Disordered Transition between the Solar Wind and the Magnetosphere, W. Bernstein, R. W. Fredricks and F. L. Scarf, J.G.R. 69, 1201 (1964).

2. Electron Acceleration and Plasma Instabilities in the Transition Region, F. L. Scarf, W. Bernstein and R. W. Fredricks, J.G.R. 70, 9 (1965).

3. Numerical Estimates of Superthermal Electron Production by Ion Acoustic Waves in the Transition Region, R. W. Fredricks, F. L. Scarf and W. Bernstein, J.G.R. 70, 21 (1965).

4. Conductive Heating of the Solar Wind, II. The Inner Corona, F. L. Scarf and L. Noble, Ap. J., May 15, 1965.

5. Preliminary Report on the Detection of Electrostatic Ion Waves in the Magnetosphere, F. L. Scarf, G. M. Crook and R. W. Fredricks, J.G.R. 70, July 1, 1965.

6. Direct Detection of Ambient Electron Plasma Oscillation Fields in the Magnetosphere, F. L. Scarf and R. W. Fredricks, J. Plan. Sp. Sci., in press.

7. On the Role of Ion Acoustic Waves in the Transition Region, F. L. Scarf, in The Solar Wind, Ed. R. Mackin, Jr., Pergamon Press, in press.

8. Effects of Solar Wind Composition on the Threshold for Plasma Instability in the Transition Region, R. W. Fredricks and F. L. Scarf, submitted to J.G.R. (see Appendix A).

9. Production of Superthermal Electrons by Electrostatic Plasma Oscillations, R. W. Fredricks, revised version to be submitted to Phys. Fluids (see Appendix B).

Published Abstracts Generated under NASw-698:

1. Plasma Instabilities in the Magnetopause, F. L. Scarf, W. Bernstein and R. W. Fredricks, Trans. A.G.U. 44, 880 (1963).

2. Transport Phenomena in the Solar Corona and Solar Wind, F. L. Scarf and L. Noble, Trans. A.G.U. 45, 78 (1964).

3. A Possible Interpretation of the P-11 VLF Measurements, F. L. Scarf and R. W. Fredricks, Trans. A.G.U. 45, 598 (1964).

4. Superthermal Electron Production in the Transition Region, R. W. Fredricks, F. L. Scarf and W. Bernstein, Trans. A.G.U. 45, 630 (1964).

5. Further Analysis of VLF Electric Field Measurements above the Ionosphere, F. L. Scarf, G. M. Crook and R. W. Fredricks, Trans. A.G.U. 46, 114 (1965).

6. Conditions for Ion Wave Instability in the Transition Region using Experimental Velocity Distribution Functions, R. W. Fredricks, F. L. Scarf and W. Bernstein, Trans. A.G.U. 46, 114 (1965).

Publications Supported Partially by NASw-698:

1. Whistler Determination of Electron Energy and Density Distributions in the Magnetosphere, H. B. Liemohn and F. L. Scarf, J.G.R. 69, 1201 (1964).

2. Dynamics of the Solar Wind, F. L. Scarf and L. Noble, AIAA Journal 2, 1158 (1964).

3. The Solar Wind and Its Interaction with Magnetic Fields, F. L. Scarf in Space Physics, Ed. D. LeGalley and A. Rosen, Wiley, 1964, p. 437.

4. The Origin of the Solar Wind, F. L. Scarf in <u>The Solar Wind</u>, Ed. R. Mackin, Jr., Pergamon Press, in press.

Miscellaneous

1. Theoretical Interpretation of Bow Shock Measurements, F. L. Scarf, invited talk at NASA/Ames - Stanford University, Conference on the Collisionless Shock, March 1-3, 1965 -- no published abstract.

2. Seminar talks at USC, Cal. Tech., JPL, Los Alamos, Stanford University, Aerospace Corp., NASA/Ames.

EFFECTS OF SOLAR WIND COMPOSITION ON THE THRESHOLD
FOR PLASMA INSTABILITY IN THE TRANSITION REGION

by

R. W. Fredricks and F. L. Scarf
TRW Space Technology Laboratories, Redondo Beach, California

2 7 7 6

The effect of a small concentration of solar wind alpha particles on the conditions for drift instability in the transition region is investigated. It is shown that for alpha particle concentrations less than about 20 percent, the proton-electron threshold curve is sufficiently accurate, for the range of relative electron-proton-alpha particle drift speeds of interest. Recent transition region plasma measurements are interpreted in terms of the conditions for marginal stability with respect to electrostatic plasma oscillations.

I. INTRODUCTION

In a recent series of papers (Bernstein, et.al., 1964; Scarf, et.al., 1965; Fredricks, et.al., 1965), the consequences of the possible existence of double-stream plasma instabilities in the transition region separating the ordered geomagnetosphere and the unperturbed solar wind were explored. In particular the lower frequency, or ion acoustic wave, branch of the double-stream plasma instability was invoked as a probable explanation for some of the phenomena observed experimentally by spacecraft instruments traversing the transition region (superthermal electrons, broad disordering of the transition, etc.).

Recent data from electrostatic analyzers aboard spacecraft (VELA, OGO-A, IMP-B) penetrating the transition region seem to indicate that the proton fluxes are significantly anisotropic in angular distribution, retaining much of their streaming energy (Wolfe and Silva, 1964; Wolfe, et.al., 1965; Strong, et.al., 1964, 1965; Bame, et.al., 1964, 1965) while electrons generally have isotropic angular distributions (Bame, et.al., 1965). The proton energy spectra often appear to have non-maxwellian tails while the portions near the mean drift energy fit a maxwellian reasonably well. The electron energy spectra are generally more maxwellian, fitting distributions for kinetic temperature from several hundred eV to more than one keV, but with small non-maxwellian high energy tails.

These recent data also indicate the presence in the solar wind of a highly variable alpha-particle content. Wolfe, et.al., (1964, 1965)

quote a range of alpha-particle to proton density in the range of zero

to perhaps eight or ten percent, while Bame, et.al. (1964, 1965) have

tentatively estimated a range of zero to perhaps twenty percent. (The

Mariner-2 electrostatic analyzer could not determine this ratio with pre-

cision.) The abundance ratios He/H reported are between 8 percent (cosmic

rays) to about 16 percent (solar system abundance), while no direct solar

abundance is available (Aller, 1961).

The critical drift velocity for marginal stability of the ion

acoustic wave was previously calculated as a function of the electron/

proton temperature ratio by Jackson (1960) and Fried and Gould (1961),

and presented graphically by Bernstein, et.al., (1964); the curve is

shown in Fig. 1. This marginal stability curve was computed under the

assumptions that the gas (1) is fully ionized, (2) is collisionless,

(3) is comprised of only electrons and protons of equal number densities,

(4) can be characterized by maxwellian electron and proton velocity dis-

tributions of kinetic temperatures T_e and T_p where $T_e \gtreqless T_p$. Hence, any

partial density of alpha particles was excluded from these previous

calculations.

In the present paper, we investigate the effect on the marginal

stability curve (critical drift velocity vs. electron/ion temperature

ratio) of small alpha particle/proton density ratios, and attempt to

relate the results to data from electrostatic analyzers on spacecraft in

the interplanetary and transition regions. It will be shown that, on the

basis of such recent spacecraft plasma data, the alpha particle content of

the solar wind can be expected to have a negligible effect on the conditions for the ion wave instabilities to occur, and that the previous marginal stability criteria (Bernstein, et.al., 1964) remain applicable to the transition region.

II. PLASMA DISPERSION RELATION

The dispersion relation governing small amplitude longitudinal waves in a homogeneous isotropic plasma having several component ion species is (Stix, 1962) for maxwellian distributions

$$1 = \sum_{j=1}^{N} \frac{4\pi n_j q_j^2 e^2}{k^2 \mathcal{K} T_j} Z'(\zeta_j - w_j) \quad , \tag{1}$$

where $Z'(\phi) = \partial Z / \partial \phi$, and $Z(\zeta_j - w_j)$ is the plasma dispersion function defined and tabulated by Fried and Conte (1961)

$$Z(\zeta_j - w_j) = \pi^{-\frac{1}{2}} \int_{-\infty}^{\infty} \left[u - (\zeta_j - w_j)\right]^{-1} \exp(-u^2) du \quad . \tag{2}$$

In (1) and (2), the symbols have the following meanings $\zeta_j = \omega/ka_j$, $w_j = v_j/a_j$, $a_j = (2\mathcal{K} T_j/m_j)^{\frac{1}{2}}$. ω and k are the angular frequency and wave number of the plasma wave, v_j is the bulk (drift) velocity of the jth ion species relative to a fixed laboratory frame, a_j is the thermal velocity of the jth species of mass m_j and kinetic temperature T_j. The quantity $\mathcal{K}$ is Boltzmann's constant, n_j is the number density and q_j the charge number of the jth species.

Bernstein and Kulsrud (1960) have shown that the dispersion relation (1) can be appropriate to ion acoustic waves even in the presence of a magnetic field. The conditions for the validity of (1) in a magnetic field are given by $\langle v^2 \rangle^{\frac{1}{2}} << c$, $\omega/|k| << c$ and $k_{\perp}\langle v^2 \rangle^{\frac{1}{2}}/\omega_c << 1$, where $\langle v^2 \rangle$ is the mean squared thermal speed, c the velocity of light, k the wave number of the perturbation, $\omega_c = eB_0/mc$ is the cyclotron frequency and $k_{\perp}$ is the projection of k perpendicular to the magnetostatic field B_0. All of these conditions appear to be readily satisfied by ion acoustic waves in the transition region.

The function defined by the Hilbert transform of the gaussian, Eq. (2), is a complex function of a generally complex argument, since for real k, the frequency ω can be complex. Equation (1) relates this complex ω to k, and thus defines the allowed spectrum of plasma oscillations. For damped or growing waves, of the type

$$E(x,t) \propto \exp(ikx - i\omega_r t) \exp(\pm \gamma t), \quad \gamma > 0 \quad ,$$

one solves (1) for $\omega = \omega_r \pm i\gamma$ at fixed values of k and the other parameters to obtain the oscillation frequency ω_r and damping or growth constant γ . This in general requires a numerical method, since (1) is a complex higher transcendental equation.

The case of marginal stability of such waves is represented by the solutions $\gamma(k) \equiv 0$ which are associated with the lowest possible normalized drift velocities $v_j/a_j = w_j$. They are examined by studying the

(graphical) solutions to (1) when $\zeta_j - w_j$ are real, as will be exemplified in our subsequent calculations. For most of the cases of practical interest, the minimum normalized drift velocities w_j will be associated with the very long wavelength modes $k \longrightarrow 0$, and it will be these modes that we shall examine in solving (1) for $\gamma = 0$. Marginal stability thus represents the boundary between growing and damped wave solutions to Eq. (1).

III. APPROXIMATE ANALYTICAL SOLUTIONS FOR MARGINAL STABILITY

Let us assume a gas of protons, alpha particles and electrons. Charge neutrality in a non-oscillatory state requires that $n_e = n_p + 2n_\alpha$. If we define the electron Debye length $\lambda_D = (K T_e/4\pi n_e e^2)^{\frac{1}{2}}$, the temperature ratios $\Theta_p = T_e/T_p$ and $\Theta_\alpha = T_e/T_\alpha$, the variable $\zeta = \omega/ka_e$, and the parameters $\xi = (\Theta_p/\delta)^{\frac{1}{2}}$, $\eta = 2(\Theta_\alpha/\delta)^{\frac{1}{2}}$, where $\delta = m_e/m_p$ is the electron/proton mass ratio ($\delta = 1/1836$), along with the density ratio $r = n_\alpha/n_p$, the dispersion relation in the ion rest frame can be written

$$2k^2 \lambda_D^2 = Z'(\zeta - w_e) + \Theta_p Z'(\xi \zeta)/(1 + 2r) + 4r\Theta_\alpha Z'(\eta \zeta)/(1 + 2r) \quad , \tag{3}$$

where we assume $w_p = w_\alpha = 0$, $w_e > 0$.

The case of no alpha particles ($r = 0$ in Eq. (3)) has been treated by Jackson (1960) and Fried and Gould (1961). The resulting minimum (critical) velocity $w_p = v_p/a_p$ vs. $\Theta_p = T_e/T_p \geq 1$ is shown in Fig. 1. We shall therefore ignore this case, and pass to those for which $r > 0$. Some limiting cases can be examined analytically rather easily, in order to ascertain roughly the effect of small alpha particle concentrations on the

w_e **vs.** Θ_p minimum velocity curve for the $\gamma(k) = 0$, $k \to 0$ solutions to (3).

A particularly simple case is that for which $T_\alpha = 4T_p$ in (3). Then $\xi = \eta$, $\Theta_p = \Theta_\alpha$ and (3) becomes

$$2k^2 \lambda_D^2 = Z'(\zeta - w_e) + \textcircled{H}_p Z'(\xi \zeta) \quad , \tag{4}$$

where the effective temperature ratio is now

$$\textcircled{H}_p = (1 + r)\Theta_p/(1 + 2r) < \Theta_p \text{ for all } 0 \leq r < \infty \quad . \tag{5}$$

One can see from Eq. (5) that in the presence of alpha particles with $T_\alpha = 4T_p$ the critical velocity curve (Fig. 1) is shifted to the right along the temperature axis, and therefore the minimum drift velocity for marginal stability computed from (4) will exceed that for $r = 0$ at any given Θ_p. This is to be expected on the basis of arguments involving the shape of the composite distribution function $F_T(v) = f_e(v) + f_p(v) + f_\alpha(v)$ in the present case. (Section 4, below).

To estimate the change in the drift velocity produced when $r > 0$, let $r = 0.1$. Then $\textcircled{H}_p = \Theta_p/1.09$, and the difference between the drift velocities is thus quite small even at $\textcircled{H}_p = 1$ ($\Theta_p = 1.09$). It decreases with increasing Θ_p. The general result can be stated as follows, where we write $w_p(\Theta_p) = a_e w_e(\Theta_p)/a_p$,

$$w_p(\Theta_p, r > 0) = w_p(\Theta_p, r = 0) + w_p' \quad , \quad 0 < w_p' << w_p(\Theta_p = 1, r = 0) \quad .$$

A second case of interest is that in which $T_\alpha = T_p \lesssim T_e$, $r \ll 1$. In this case $\theta_\alpha = \theta_p = \theta$, while $\eta = 2\xi$ in Eq. (3). If we add and subtract a quantity $\theta Z'(\xi, \zeta)$ on the r.h.s. of Eq. (3), we obtain

$$2k^2 \lambda_D^2 = Z'(\zeta - w_e) + \theta Z'(\xi, \zeta) + \frac{2r\theta}{1 + 2r} \left\{ 2Z'(2\xi, \zeta) - Z'(\xi, \zeta) \right\} , \quad (6)$$

which is in a form appropriate to perform a perturbation calculation. For very small r, the last term on the r.h.s. of Eq. (6) should yield a very small correction to the solution to (6) when $r = 0$. In particular, let us consider the well-known solution to (6) for $r = 0$, $\theta = 1$. It is shown by Fried and Gould (1961) that in this case, one has

$$\left. \begin{array}{c} \zeta - w_e = - 0.925 \\ \xi \zeta = + 0.925 \end{array} \right\} , \quad k^2 \lambda_D^2 \to 0^+, \quad \xi = \delta^{-\frac{1}{2}} , \quad (7)$$

which yields a critical drift velocity

$$w_e(\theta = 1, r = 0) = (0.925)(1 + \delta^{\frac{1}{2}}) \quad . \quad (8)$$

For $1 \gg r > 0$ let us try a solution

$$\left. \begin{array}{c} \zeta - w_e = - 0.925 + \epsilon_1 \\ \xi \zeta = + 0.925 + \epsilon_2 \end{array} \right\} , \quad (9)$$

where ϵ_1 and ϵ_2 are real, small first order quantities depending on r such that terms proportional to products of the type ϵ_1^2, ϵ_2^2, $\epsilon_1 \epsilon_2$, $\epsilon_1 r$ and $\epsilon_2 r$ can be neglected. Then to first order, a Taylor's series expansion of Eq. (6) about the points $\zeta - w_e = - 0.925$ and $\xi \zeta = + 0.925$ yields for $\theta = 1$

$$\underset{k \to 0}{\text{Lim}} \; 2k^2 \lambda_D^2 = Z'(-0.925) + Z'(+0.925) + \epsilon_1 Z''(-0.925) + \epsilon_2 Z''(+0.925)$$

$$+ \frac{2r}{1 + 2r} \left[2Z'(1.85) - Z'(0.925) \right] \quad . \tag{10}$$

Now the function $Z'(x)$ for real x can be written (Fried and Conte, 1961),

$$Z'(x) = 2 \left[2x^2 \; Y(x) - 1 \right] - i2\pi^{\frac{1}{2}} x \exp(-x^2) \quad , \tag{11}$$

where

$$Y(x) = x^{-1} \exp(-x^2) \int_0^x \exp(u^2) \; du \quad . \tag{12}$$

It follows that $Z'(x)$ has the symmetry properties,

$$\left. \begin{array}{l} \text{Re } Z'(x) = \text{Re } Z'(-x) \\[2mm] \text{Im } Z'(x) = - \text{Im } Z'(-x) \end{array} \right\} \quad , \tag{13}$$

while the second derivative $Z''(x)$ has the properties,

$$\left. \begin{array}{l} \text{Re } Z''(x) = - \text{Re } Z''(-x) \\[2mm] \text{Im } Z''(x) = \text{Im } Z''(-x) \end{array} \right\} \quad . \tag{14}$$

The real part of $Z'(x)$ vanishes at $x = \pm 0.925$. Hence, by use of (13) it can be seen that the first two terms on the r.h.s. of Eq. (10) vanish identically. If we pass to the limit $k^2 \lambda_D^2 \to 0^+$, then the real and imaginary parts of Eq. (10) yield two inhomogeneous algebraic equations which determine the two unknowns ϵ_1 and ϵ_2. These equations may be written

$$\left. \begin{aligned} \epsilon_1 - \epsilon_2 &= \left[4r\ \text{Re}\ Z'(1.85) \right]/(1 + 2r) \cdot \text{Re}\ Z''(0.925) \\ \epsilon_1 + \epsilon_2 &= -2r \left[\text{Im}\ Z'(1.85) - \text{Im}\ Z'(0.925) \right]/(1 + 2r) \cdot \text{Im}\ Z''(0.925) \end{aligned} \right\} \quad , $$

$$(15)$$

where use was made of relations (13) and (14). The function $Z(x)$ satisfies the differential relation

$$Z''(x) = (2/x) - (2x - 1/x)\ Z'(x) \quad , $$

and the numerical coefficients in (15) may be obtained using the tabulated values of $Z'(x)$ given by Fried and Conte (1961):

$$4\ \text{Re}\ Z'(1.85/\text{Re}\ Z''(0.925) \doteq 0.880 $$

$$2 \left[(\text{Im}\ Z'(1.85) - \text{Im}\ Z'(0.925) \right]/\text{Im}\ Z''(0.925) \doteq 1.79 \quad . $$

This yields

$$\left. \begin{aligned} \epsilon_1 - \epsilon_2 &= 0.88r/(1 + 2r) \\ \epsilon_1 + \epsilon_2 &= 1.79r/(1 + 2r) \end{aligned} \right\} \quad , \qquad (16)$$

so that

$$\left. \begin{aligned} \epsilon_1 &= -\ 0.455r/(1 + 2r) \\ \epsilon_2 &= -\ 1.335r/(1 + 2r) \end{aligned} \right\} \quad . \qquad (17)$$

Equation (9) may be solved for the drift velocity w_e,

$$w_e(\Theta = 1,\ r > 0) = 0.925(1 + \delta^{\frac{1}{2}}) + (0.455 - 1.355\delta^{\frac{1}{2}})r/(1 + 2r) \quad , $$

$$(18)$$

and, since $\delta^{\frac{1}{2}} = (m_e/m_p)^{\frac{1}{2}} = 1/42.85$, $w_e(\Theta = 1, r = 0) = 0.925(1 + \delta^{\frac{1}{2}})$,

we finally obtain

$$w_e(\Theta = 1, r > 0) = w_e(\Theta = 1, r = 0) + 0.424r/(1 + 2r) \quad . \quad (19)$$

Therefore, in this case $(T_\alpha = T_p, \; 0 < r \ll 1$ and $v_\alpha = v_p)$ the presence of

an alpha particle concentration leads to a slightly higher drift velocity

for marginal stability than that required in the case of no alpha particles,

$r = 0$. We shall show in a subsequent section that the result (19) for

$\Theta = 1$ holds for all $\Theta > 1$. Numerical values of the shift in required

drift velocity can be computed for, say, $r = 0.1$. They yield

$$w_e(\Theta = 1, \; r = 0.1) - w_e(\Theta = 1, \; r = 0) = 0.0355,$$

which yields an equivalent proton drift velocity shift of

$$v_p(\Theta = 1, \; r = 0.1) - v_p(\Theta = 1, \; r = 0) = 1.52a_p = 1.52(2K\,T_p/m_p)^{\frac{1}{2}} \quad .$$

A natural question to ask at this point is: what would be the

effect on the minimum critical drift velocity for marginal stability of

the presence of alpha particles drifting with respect to both the protons

and electrons? To examine this case, let us work in the electron rest

frame $w_e = 0$, and set $T_\alpha = T_p$, $w_\alpha = (1 + \sigma)w_p$. The convenient variable in

Eq. (1) then becomes $\zeta = \omega/ka_p$. In this variable, Eq. (1) can be written

in a form analogous to Eq. (6),

$$2k^2 \lambda_D^2 = Z'(\delta^{\frac{1}{2}}\Theta^{-\frac{1}{2}}\zeta) + \Theta Z'(\zeta - w_p) + \frac{2r\Theta}{1 + 2r}\left[2Z'(2\zeta - 2w_p - 2\sigma w_p) - Z'(\zeta - w_p)\right].$$

$$(20)$$

As in the treatment of (6), let us seek solutions to (20), for very small r and $\Theta = 1$, in the form

$$\delta^{\frac{1}{2}} \zeta = + 0.925 + \epsilon_3$$

$$\zeta - w_p = - 0.925 + \epsilon_4$$

$$2(\zeta - w_p) - 2\sigma w_p = - 1.85 + 2\epsilon_4 - 2\sigma w_p \approx - 1.85 - 2\sigma w_p \tag{21}$$

A Taylor's series expansion of (20) yields

$$2k^2 \lambda_D^2 \rightarrow 0^+ = Z'(0.925) + Z'(-0.925) + \epsilon_3 Z''(0.925) + \epsilon_4 Z''(-0.925)$$

$$+ \frac{2r}{1 + 2r} \left[2Z'(-1.85 - 2\sigma w_p) - Z'(-0.925) \right] \quad . \tag{22}$$

If Eq. (13) and (14), are used again, we obtain the two equations determining ϵ_3 and ϵ_4,

$$\left.\begin{array}{l} \epsilon_3 - \epsilon_4 = - fr/(1 + 2r) \\[2mm] \epsilon_3 + \epsilon_4 = gr/(1 + 2r) \end{array}\right\} \tag{23}$$

where

$$f = 4\mathrm{Re}Z'(1.85 + 2\sigma w_p)/\mathrm{Re}Z''(0.925)$$

$$g = 2 \left\{ 2\mathrm{Im}Z'(1.85 + 2\sigma w_p) - \mathrm{Im}Z'(0.925) \right\}/\mathrm{Im}Z''(0.925) \quad . \tag{24}$$

The solutions to (23) are

$$\epsilon_3 = \tfrac{1}{2}(g - f)r/(1 + 2r), \quad \epsilon_4 = \tfrac{1}{2}(g + f)r/(1 + 2r) \quad . \tag{25}$$

These values of ϵ_3 and ϵ_4 yield the new drift velocity

$$w_p = 0.925(1 + \delta^{\frac{1}{2}}) + \tfrac{1}{2} \left[(g - f)\delta^{-\frac{1}{2}} - (g + f) \right] r/(1 + 2r) \quad . \tag{26}$$

The first term on the r.h.s. of (26) is just the value of critical drift velocity in the case $r = 0$, $\Theta = 1$. If drifting alpha particles are to reduce the required drift below the value for $r = 0$, then the coefficient of $r/(1 + 2r)$ in Eq. (25) must be negative, which requires

$$(\delta^{-\frac{1}{2}} + 1)f \ge (\delta^{-\frac{1}{2}} - 1)g \quad . \tag{27}$$

This places a condition on the magnitude of σ . Actually, we may treat Eq. (27) as a transcendental equation (or inequality) and solve it for the variable $x = 1.85 + 2\sigma w_p$. If the equality sign in (27) is taken and the numerical values of the functions appearing in (24) are used, as well as the value $\delta^{-\frac{1}{2}} = 42.85$, the equation becomes

$$\text{Re } Z'(x) - 1.93020 \text{ Im } Z'(x) = 1.34437 \quad . \tag{28}$$

We have solved this equation graphically, and obtain

$$x = 1.850 + 2\sigma_c w_p = 1.686 \quad .$$

Therefore

$$\sigma_c = -0.082/w_p \quad . \tag{29}$$

The magnitude of σ_c can be estimated by using the value of normalized drift velocity $w_p = w_p(\Theta = 1, r = 0) = 0.925(1 + \delta^{-\frac{1}{2}}) = 40.56$, and (29) yields $\sigma_c \sim -2.02 \times 10^{-3}$. If σ becomes more positive than this value, the effect of the alpha particle drift will be to raise the drift velocity required for marginal stability above the value required when $r = 0$. We find from (29) that the alpha particles can lower the drift velocity for marginal

stability only if they are drifting somewhat more slowly than the protons. However, since the perturbation calculation based on Eq. (20) cannot be extended to include large negative values of σ , it is dangerous to conclude that the critical drift velocity w_p can be continuously lowered if we make σ very much more negative than the value -2.02×10^{-3}. It will be shown in the next section that when the difference between proton and alpha particle drift velocity is on the order of several proton thermal velocities, that is $v_p - v_\alpha = Na_p$, $N \gtrsim 2$, their effects in Eq. (20) become decoupled, and that for density ratios $0 \leq r < 0.2$ of interest to us in considering solar wind effects, the alpha particles have no influence on the proton drift velocity required to produce states of marginal stability of ion acoustic waves.

IV.   TOTAL DISTRIBUTION FUNCTIONS AND MARGINAL STABILITY

A double stream instability occurs in a plasma having a total particle distribution function $F_T(v) = \sum_j f_j(v)$ only if $F_T(v)$ possesses several peaks, or relative maxima and minima, of the proper type. There are conditions on the separations of the relative maxima, on the magnitudes of these maxima and the change in slope near the relative minima (Penrose, 1960). Consider, for example, the composite maxwellian distribution

$$\pi^{\frac{1}{2}} F_T(v) = n_e a_e^{-1} e^{-v^2/a_e^2} + n_p a_p^{-1} e^{-(v-v_p)^2/a_p^2} + n_\alpha a_\alpha^{-1} e^{-(v-v_\alpha)^2/a_\alpha^2} \quad ,$$

$$(30)$$

which represents a non-drifting electron distribution and drifting proton and alpha particle distributions. This function is sketched in Fig. 2 for a case $T_e >> T_p \sim T_\alpha$, and two cases of drift: either $v_\alpha < v_p$ or $v_\alpha > v_p$. It is easy to show by numerically evaluating Eq. (30) in this case that if $v_\alpha = v_p \pm N a_p$, where $N \gtrsim 2$, then for density ratios $0 < r < 0.2$ the alpha particles will not noticeably influence the relationship between $f_e(v)$ and $f_p(v)$ which determines the instability. In this case the relative distributions in the vicinity of $v = v_p$ are

$$f_p(v_p) = n_p a_p^{-1}$$

$$f_\alpha(v_p) = n_\alpha a_\alpha^{-1} \exp\left[-N^2 a_p^2 / a_\alpha^2\right] \qquad ,$$

and the ratio

$$f_\alpha(v_p)/f_p(v_p) = (n_\alpha/n_p)(a_p/a_\alpha) \exp\left[-N^2 a_p^2/a_\alpha^2\right] ,$$

becomes

$$f_\alpha(v_p)/f_p(v_p) = 2r \exp(-4N^2) < 0.4e^{-16} \qquad ,$$

for $T_\alpha = T_p (a_p = 2a_\alpha)$, $N \gtrsim 2$.

Since this ratio is less than or on the order of 10^{-8}, we see the nearly null influence of the drifting alpha particles. Thus, the approximate treatment of (20) will not be valid for large negative σ.

In order to understand the influence of $f_\alpha(v)$ on the criterion for instability when $v_\alpha \approx v_p$, consider the graphical representation in Fig. 3, where we have plotted the gaussian $f_p(v)$ centered at v_p, and the two gaussians $f_\alpha^{(+)}_{(-)}(v)$ centered at $v_p \pm a_p/2$. The additions of the dashed curves $f_p(v)$ and $f_\alpha^{+}(v)$, are the solid curves. We note that the distribution derived by adding the small gaussian centered at $v_p - a_p/2$ shifts

the peak of the composite curve to the left, i.e., to $v_p - v_p'$. It also decreases the "apparent temperature" on the ℓ.h.s. of the curve, by steepening the slope. Since a steeper slope on this side of the composite distribution, when intersecting a non-drifting hot electron distribution as in Fig. 2, tends to decrease stability (Penrose, 1960), the reason for the result (29) derived by perturbation of the $r = 0$ dispersion relation can be seen. The case in which $f_\alpha(v)$ peaks at $v_p = a_p/2$ will lead to increased stability by reversal of the arguments just presented to explain decreased stability.

V.   GRAPHICAL SOLUTIONS TO THE DISPERSION RELATION

As was previously stated, the dispersion relation (1) is a transcendental equation containing the two variables ω and k and many parameters such as densities, temperatures, masses, etc. Solutions to (1) using purely analytical methods appear impossible; it is therefore necessary to solve (1) for ω and k by either numerical machine computation, or by a suitable graphical technique. We shall present one of the latter methods which is simple and relatively rapid if one wishes to compute the drift velocity vs. temperature ratio for ion acoustic wave marginal stability. The technique has been used previously by Jackson (1960).

Let us first put the dispersion relation into a suitable form. In the electron rest frame, $w_e = 0$, (1) may be written in the form

$$2k^2 \lambda_D^2 = Z'(\phi_1) + \frac{\theta}{1 + 2r} \left[Z'(\phi_2) + 4r \, Z'(\phi_3) \right] \quad , \tag{31}$$

where we study the case $T_\alpha = T_p = T_i$, $\Theta = T_e/T_i \gtrsim 1$. The arguments of the dispersion functions are $\phi_1 = \omega/ka_e$, $\phi_2 = (\omega/k - v_p)a_p$, $\phi_3 = (\omega/k - v_\alpha)/a_\alpha$. For purposes of studying a specific numerical example, let us choose $r = 0.1$, corresponding to a solar wind condition in which the alpha particle-to-proton content is 10 percent. Also, let us rewrite ϕ_3 in terms of the variable ϕ_2. Since $a_\alpha = a_p/2$, the relationship

$$\phi_3 = 2(\omega/k - v_p)a_p \overset{-}{+} 2|v_1| a_p$$

$$= 2\phi_2 \overset{-}{+} \Delta \quad , \quad \Delta = 2|v_1|/a_p \geq 0 \quad ,$$

applies with $v_\alpha = v_p \overset{+}{-} |v_1|$. Since $1 + 2r = 1.2$, the new function

$$G'(\phi_2 ; \Delta) = \frac{\Theta}{1.2}\left[Z'(\phi_2) + 0.4 \, Z'(2\phi_2 \overset{-}{+} \Delta) \right] , \qquad (32)$$

may be defined and (31) becomes

$$2k^2 \lambda_D^2 = Z'(\phi_1) + G'(\phi_2; \overset{-}{+}\Delta) \quad . \qquad (33)$$

For the long wavelength, marginally stable modes, we allow $k^2 \lambda_D^2 \to 0^+$ in (33), and obtain the two equations

$$\left.\begin{aligned}
\text{Re } Z'(\phi_1) &= -\text{Re } G'(\phi_2; \overset{-}{+} \Delta) \\
\text{Im } Z'(\phi_1) &= -\text{Im } G'(\phi_2; \overset{-}{+} \Delta)
\end{aligned}\right\} . \qquad (34)$$

From the symmetry properties (13) of the plasma dispersion function, it can be shown that (34) will be satisfied by the pair of points

$$(\phi_1 = P_1, \ \phi_2 = - P_2) \qquad ,$$

where P_1 and P_2 are positive real numbers. To find these points, we plot the trajectories of the functions $Z'(\phi_1)$ and $G'(\phi_2)$ with ϕ_1 and ϕ_2 as parameters. The function $Z'(\phi_1)$ on the complex Z'-plane is shown in Fig. 4. The ordinate is $\text{Im } Z'(\phi_1)$ and the abscissa is $\text{Re } Z'(\phi_1)$. For $\phi_1 > 0$, $Z'(\phi_1)$ lies entirely in the lower half-plane. (The function for $\phi_1 < 0$ is the reflection across the real axis). Thus, the function Z' in Fig. 4 is the r.h.s. of (34). If $-G'(\phi_2)$ is plotted on the same scale for $\phi_2 < 0$, it will lie also in the lower half plane. The intersection $\phi_1 = P_1$, $\phi_2 = -P_2$ of the trajectories $Z'(\phi_1)$ and $-G'(\phi_2)$ yields the solution to (34) for a specified value of the parameter Δ in (32). These two trajectories can be plotted with the aid of the numerical tables of $Z'(\phi)$ for real (positive or negative) values of ϕ.

We note that the function $G'(\phi_2)$ as defined by Eq. (32) contains the temperature ratio $\Theta = T_e/T_i$ as a multiplicative, or scaling, factor. As Θ increases, the trajectory $-G'(\phi_2)$ expands without changing shape. This behavior results in intersections $\phi_1 = P_1 \rightarrow 0$, $\phi_2 = -P_2 \rightarrow \infty$, a steadily decreasing drift velocity v_p as $\Theta \rightarrow \infty$. However, since the state of marginal stability is defined such that it involves the <u>minimum</u> of all possible drift velocities which reduce the damping to zero ($\gamma(k) = 0$), one reaches a point $\phi_1 = P_1^*$, $\phi_2 = -P_2^*$ at which the $k \rightarrow 0$ mode is not associated with the <u>minimum</u> drift velocity, but rather some mode $k > 0$, i.e., $k^2 \lambda_D^2 \neq 0$ in (31) will yield a minimum drift velocity (Jackson, 1960; Fried and Gould, 1961). This occurs for $\Theta \gtrsim 20$, and is of no interest to us here.

As specific examples in Figs. 5, 6 and 7 the graphical intersections defining the solutions to (34) are shown for the cases $v_\alpha - v_p = + a_p/2$, $v_\alpha - v_p = 0$, $v_\alpha - v_p = - \frac{a}{2}p$ ($\Theta = 1.2$). The critical drift velocities for the case $\Theta = 1.2$, $r = 0.1$ and a range of relative proton-alpha particle drifts are sketched in Fig. 8. This curve was computed from the graphically determined intersections $\emptyset_1 = P_1$, $\emptyset_2 = P_2 (P_1, P_2 > 0)$ using the formula

$$w_p = P_2 + a_e P_1 / a_p = P_2 + 46.94 P_1 \quad ,$$

and may be compared with the value $w_p (\Theta = 1.2, r = 0) = 39.07$ for the case in which no alpha particles are present (dashed horizontal line in Fig. 8).

After a systematic study of the graphical solutions for a wide range of temperature ratios Θ and relative proton-alpha particle drift speeds ($w_p - w_\alpha$), one concludes that when the alpha particle concentration is in the range 0 to 20 percent, there will be little difference from the minimum critical drift velocity for marginal ion acoustic wave stability as plotted in Fig. 1. Whatever difference occurs in this curve due to alpha particle content and relative drift is almost certain to be negligible when compared with perturbing effects from ion density gradients, possible anisotropies in the plasma, magnetic field gradients, etc.

VI.   DISCUSSION

To the extent that the particle distribution functions are maxwellian and that the ion oscillation wave numbers satisfy the criterion, $k_\perp a/\omega_c \ll 1$,

etc., it has been shown that the threshold curve of Fig. 1 should be applicable in the transition region for $r \ll 1$. The recent electrostatic analyzer measurements on Vela 2A, Vela 2B, OGO-A, IMP-B suggest that a distinct intermediate state with warm streaming protons and hot electrons does indeed form in the transition region, and it is tempting to interpret this as a state of marginal stability with respect to electrostatic plasma oscillations.

In the outer transition region the proton analyzers typically detect either the cool, highly streaming protons associated with the solar wind $(v_p^{(o)} \simeq 300\text{-}700$ km/sec, $K T_p^{(o)} \simeq 10\text{-}30$ ev), or a somewhat hotter and slower proton stream $(v_p' \simeq (0.6\text{-}0.9)v_p^{(o)}$, $K T_p' \simeq (3\text{-}5)$ $K T_p^{(o)})$ with a non-maxwellian tail which tends to flow around the magnetosphere. The measurements indicate that the spectrum "hops" back and forth between these two states in the outer transition region, but that the plasma generally "settles" into the broader state within two earth radii of the magnetosphere boundary. In the electron mode, the Vela analyzers generally detect isotropic distributions with $10^{6\,o}K < T_e < 3 \times 10^{8\,o}K$. The higher temperatures are found near the 17 R_e magnetospheric boundary and the Explorer 12 CDSTE response (Freeman, 1964) also indicates that large fluxes of kilovolt electrons are present just beyond the magnetopause.

The most plausible explanation for the "hopping" in the outer transition region is that the region contains filaments with two plasma states which the spacecraft encounters alternately as it moves along

its trajectory. $\Big[$ The very large amplitude, short-period magnetic pulses observed on Pioneer I (Sonett and Abrams, 1963, Figs. (3) - (10)) and Explorer 12 (Cahill and Amazeen, 1963, Fig. (3) may be solitary waves which propagate upstream and trigger the drift instability causing filaments of the second plasma state; kinematic considerations then suggest that, on the average, the most distant upstream magnetic disturbances should be located near the fluid dynamic "shock" boundary. $\Big]$ If the second or "warm" plasma state is indeed one of the marginal stability, then in the electron rest frame, rough equipartition of mechanical energy yields $N_p'(\frac{1}{2}m_p v_p'^2 + \frac{5}{2} K T_p') \sim \frac{5}{2} Ne' K T_e'$, so that $T_e'/T_p' \gg 1$ and $\frac{1}{2}m_p v_p'^2 \sim 16 K T_p'$ (See Fig. 1). Peak ion wave potentials as large as $0.35(m_p v_p^{(o)2}/2)$ (Stix, 1964) may then be anticipated.

As noted above, the analyzer results do indicate that $T_e' \gg T_p'$ in the transition region and these observations are also reasonably consistent with the stability condition $v_p' \sim 4(2 K T_p'/m_p)^{\frac{1}{2}}$. No direct transition region measurements of ion wave potentials have been made, but the presence of spikes of superthermal electrons ($E > 40$ keV) can indicate that peak potentials on the order of hundreds of volts develop, as discussed by Scarf, et.al., (1965), Fredricks, et.al., (1965). However, these early comparisons are subject to several uncertainties, and no unambiguous identification with a state of marginal stability can be made at this time. For instance, although electron angular distributions are generally fairly isotropic in the inner transition region, it is not yet possible to determine with any accuracy the extent to which the electron rest frame

differs from the spacecraft frame of reference. An even more serious problem is related to the possibility that hypothetical large amplitude electrostatic oscillations may introduce biases into operation of plasma probes. Although this aspect of the plasma instability is relatively unexplored, there is some reason to believe that the averaged response from the electrostatic analyzers on Vela 2A, 2B, OGO-A and IMP-B is not seriously contaminated by such oscillations. In particular, simultaneous time-averaged (transition region) positive ion measurements from Vela 2A, OGO-A and IMP-B yield points which fit remarkably well with a single proton-alpha particle spectrum (J. H. Wolfe, S. J. Bame and I. B. Strong, private communication). Since the analyzers have different energy ranges, energy windows, angular aperatures, switching and sampling times, etc., and since they are located on spacecraft of greatly varying physical sizes and shapes, this correspondence is quite significant. The OGO-A and Vela analyzers measure essentially D.C. proton fluxes down to 300 ev; the agreement then indicates that any serious contamination affects only protons with lower energies, that it is of such a nature that it does not register on analyzers with long time constants, or that it disappears when the instantaneous analyzer response is averaged over several sampling cycles.

Finally, it is worth noting that the drift instability discussed above is readily produced in the laboratory when charge separation electric fields are imposed on collisionless plasmas with $T_e/T_i \gg 1$. Figure 9(a) shows the energy spectrum of a stable cold ($T_i \approx 100^\circ K$) cesium beam while

it is being neutralized by $3000^{\circ}K$ electrons (Sellen and Shelton, 1961). The neutralization is deliberately non-uniform so that significant electric fields are present throughout the system. When the neutralization is nearly complete (i.e., when the beam becomes a plasma), the ion spectrum suddenly broadens and shifts to a somewhat lower mean streaming energy (Fig. 9(b)); at the same time the electrons gain additional thermal energy (determined by the emission spectrum of cesium atoms and ions) and large amplitude, low frequency space charge oscillations occur (determined by deflection of an electron beam probe and by measurement of a modulated ion current at the collector).

ACKNOWLEDGEMENTS

Figure 1. Stability diagram for a hydrogen plasma with maxwell-boltzmann distribution functions. If the relative electron-proton drift speed is greater than $u_p^{(c)}(T_e, T_i)$, the system is overstable and large amplitude electrostatic plasma oscillations develop. For $T_e/T_i \leq 20$, the $k \simeq 0$ modes grow most rapidly.
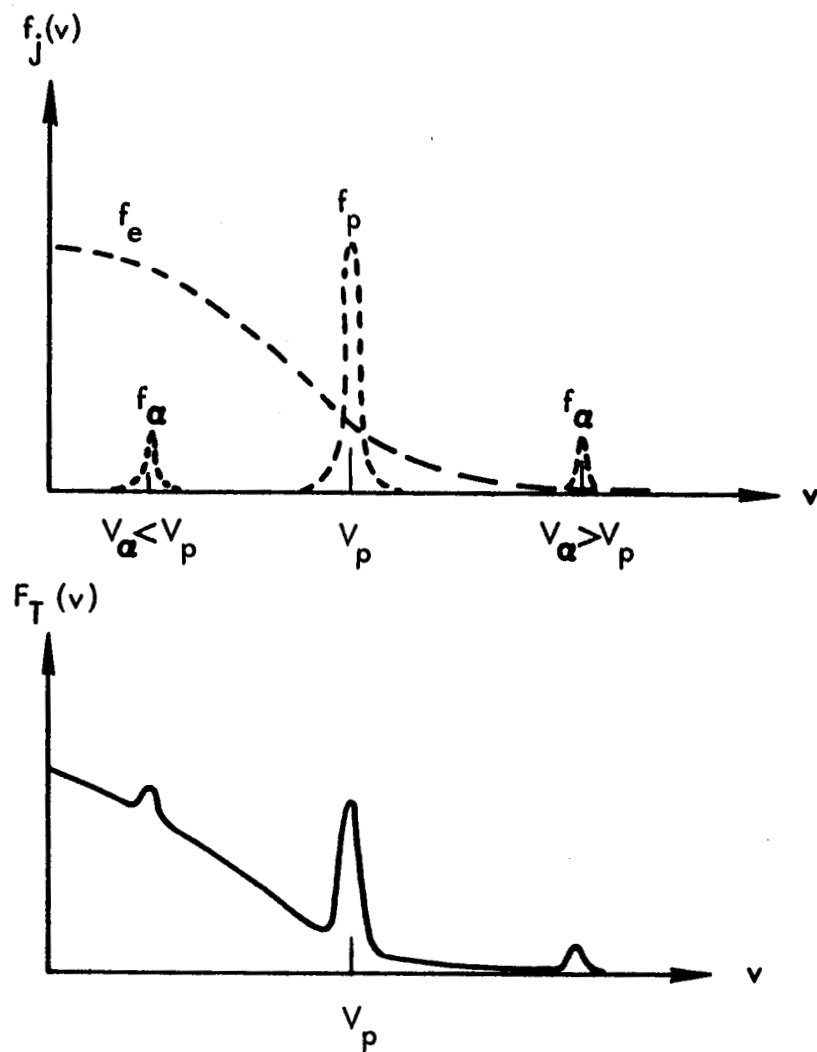
Figure 2. Composite maxwellian velocity distribution
for the case $v_e = 0$, $T_e >> T_1$, and for the
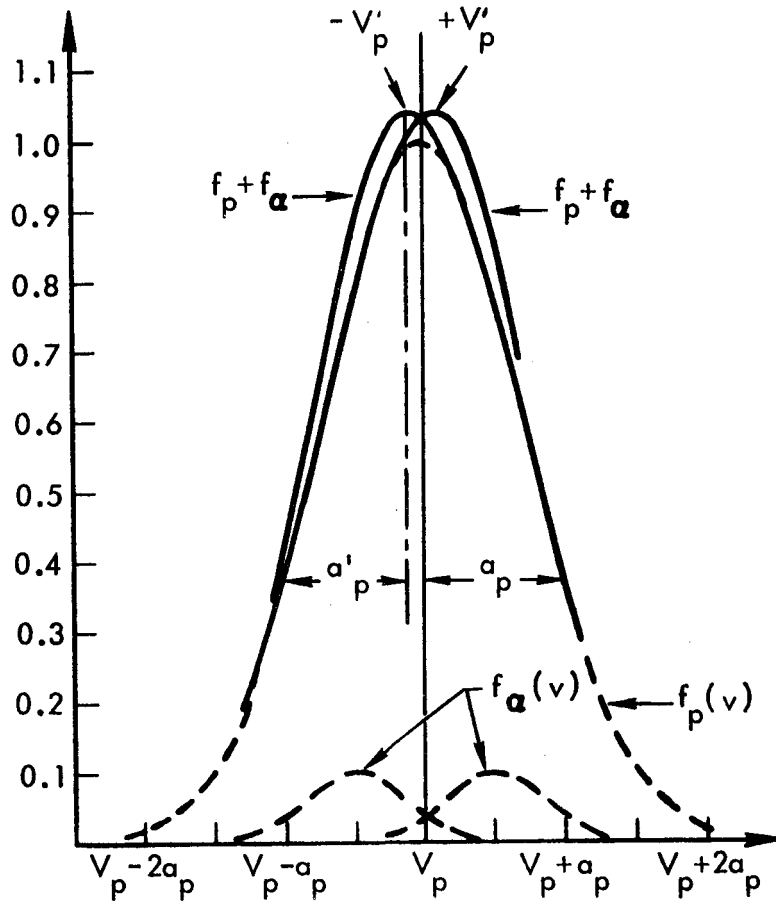two cases $v_\alpha > v_p$ and $v_\alpha < v_p$.

Figure 3. Structure of the ion distribution function when $v_\alpha \simeq v_p$, showing the shift in the peaks to $\pm v_p'$ and the change in apparent temperature to $a_p' = (2 \varkappa T_p'/m_p)^{\frac{1}{2}}$ when $v_\alpha \leqslant v_p$.
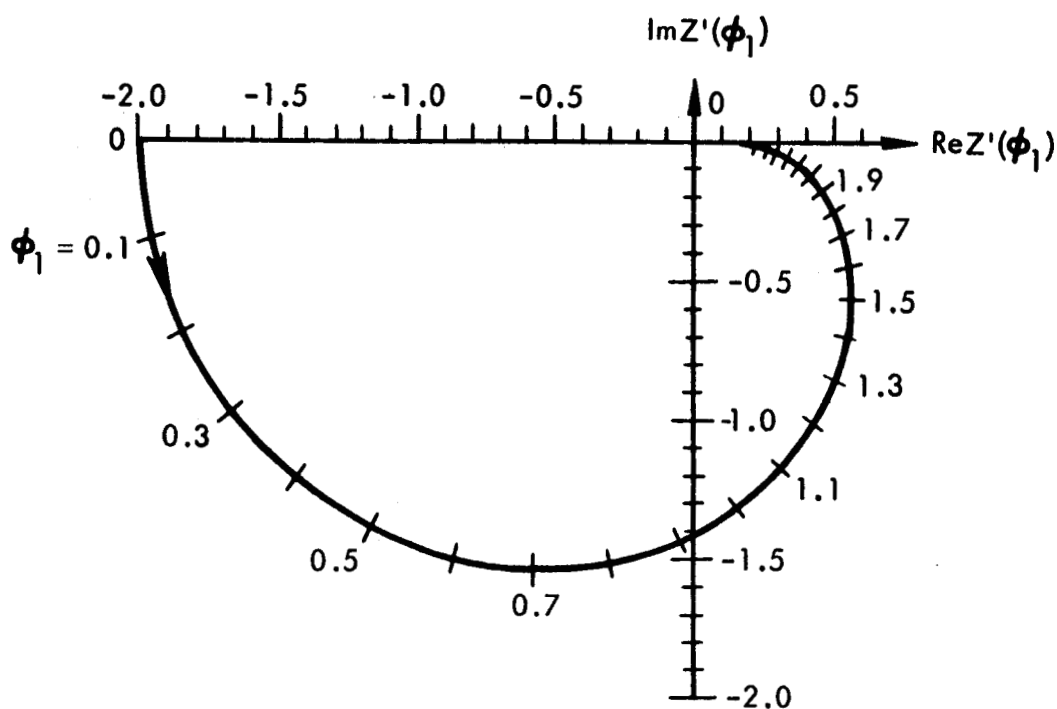
Figure 4. The plasma dispersion function $Z'(\phi_1)$ on the complex Z'-plane for ϕ_1 positive and real. For ϕ_1 negative and real, the function is reflected across the real axis. The origin corresponds to $\phi_1 = \pm \infty$.
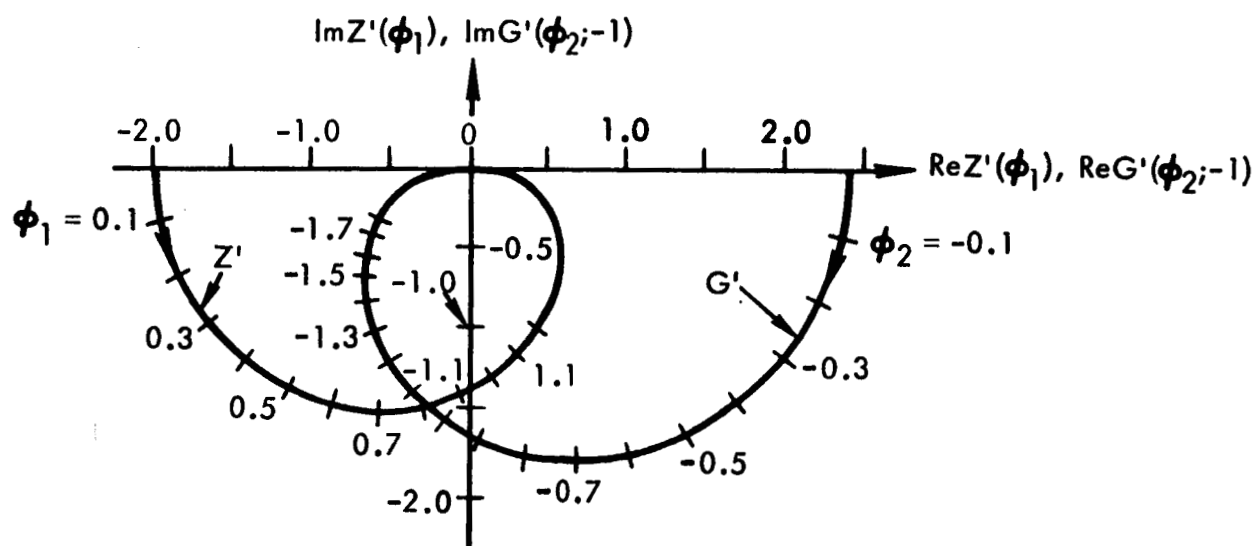
Figure 5. The intersection of the trajectories $Z'(\phi_1)$ and $G'(\phi_2)$ for a relative drift $v_\alpha - v_p = 0.5a_p$.
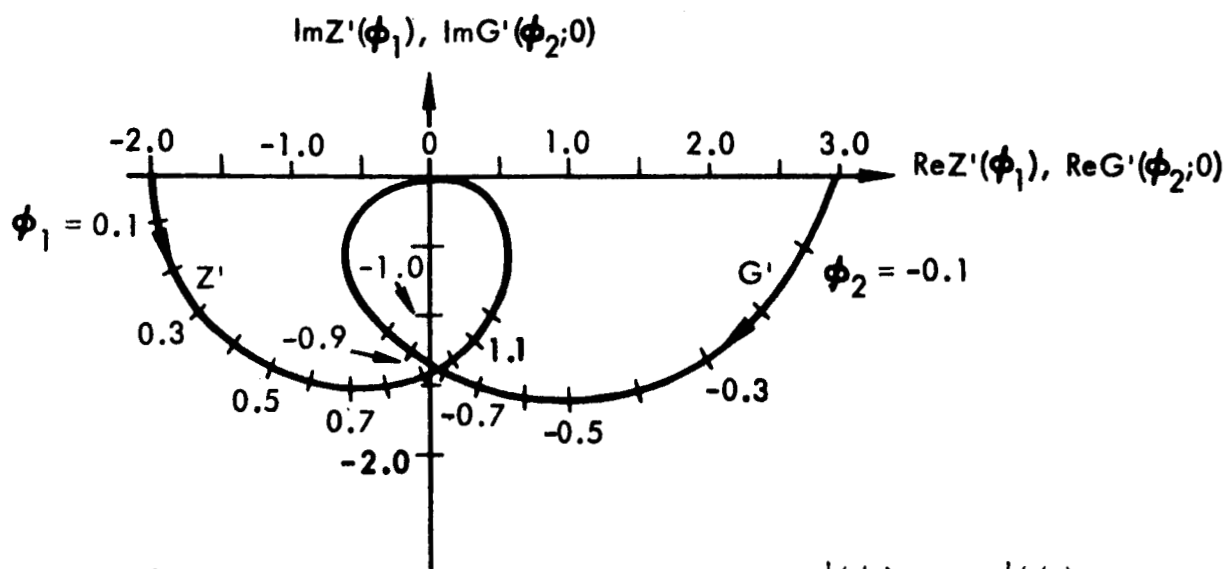
Figure 6. The intersection of the trajectories $Z'(\phi_1)$ and $G'(\phi_2)$ for a relative drift $v_\alpha - v_p = 0$.
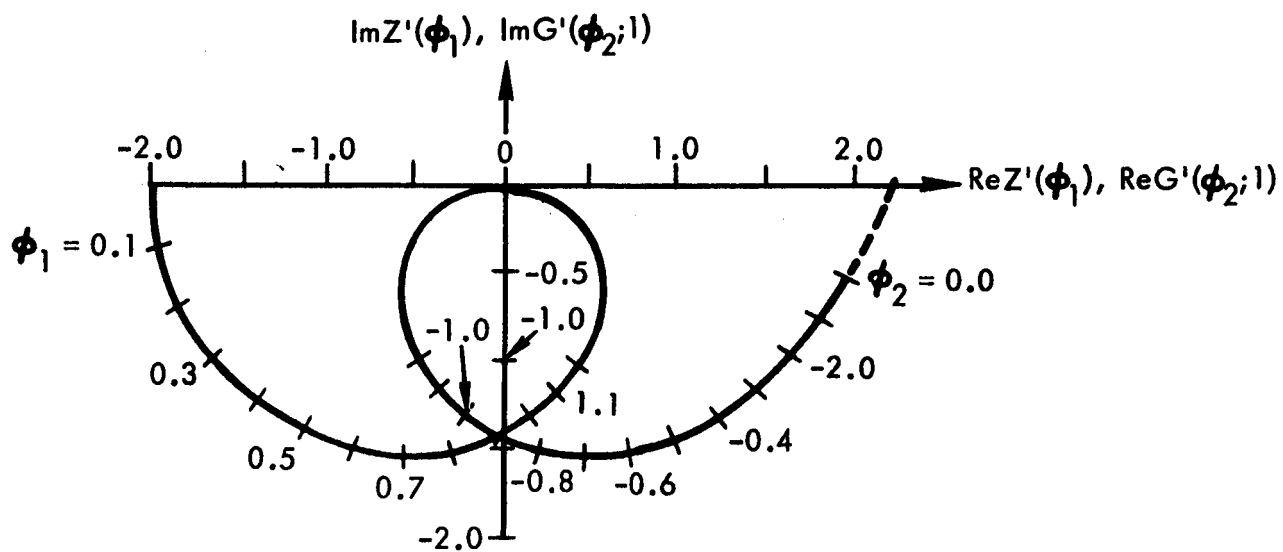
Figure 7. The intersection of the trajectories $Z'(\phi_1)$ and $G'(\phi_2)$ for a relative drift $v_\alpha - v_p = - 0.5a_p$.
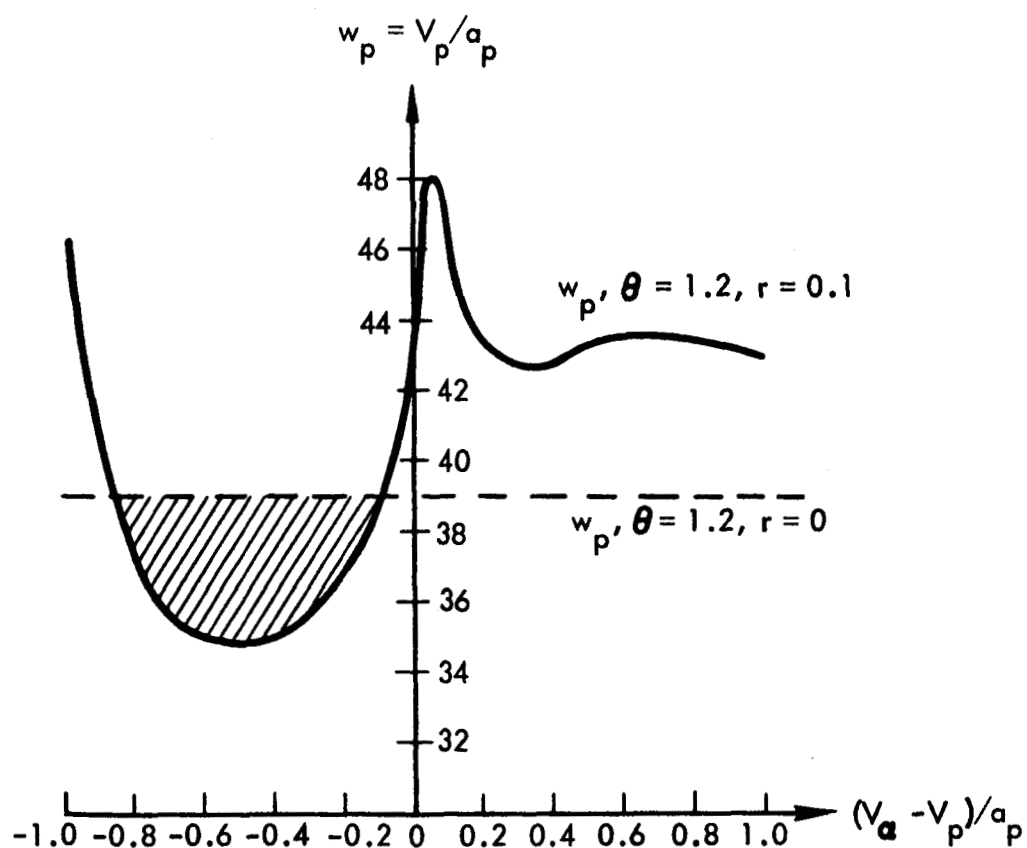
Figure 8. The critical normalized drift velocity $w_p = v_p/a_p$ for marginal stability as a function of relative proton-alpha particle drift $(v_\alpha - v_p)/a_p$.
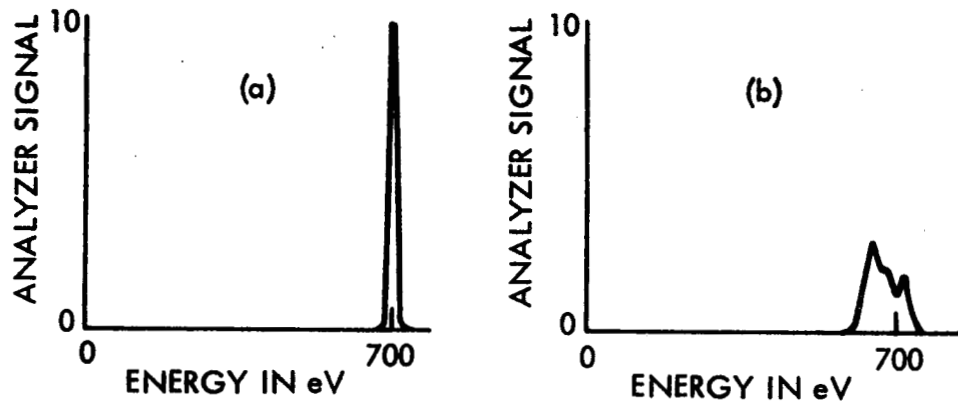
Figure 9(a). Collisionless cesium beam in non-oscillatory
state while it is being neutralized non-uniformly.

Figure 9(b). When neutralization is nearly complete, plasma
oscillations occur. The cesium spectrum is broadened
and the ions lose energy. In the oscillatory state,
hot electrons are produced and they excite spectral
lines of cesium I and cesium II. The space charge
oscillation frequency is very low in the plasma
frame of reference; in the lab frame $\omega \simeq ku_0$ with $kL \simeq 1$.

REFERENCES

Aller, L. H., *The Abundance of the Elements*, Interscience Publishers, Inc., New York, 1961.

Bame, S. J., J. R. Asbridge, H. E. Felthauser, R. A. Olsen and I. B. Strong, Characteristics of the particle activity near the dawn boundary of the magnetosphere, *Trans. Am. Geophys. Union*, 46, 142, 1965.

Bernstein, I. B. and R. M. Kulsrud, Ion wave instabilities, *Phys. Fluids*, 3, 937, 1960.

Bernstein, W., R. W. Fredricks and F. L. Scarf, A model for a broad dis-ordered transition region between the solar wind and the magnetosphere, *J. Geophys. Res.*, 69, 1201, 1964.

Cahill, L. J. and P. G. Amazeen, The boundary of the geomagnetic field, *J. Geophys. Res.*, 68, 1835, 1963.

Fredricks, R. W., F. L. Scarf and W. Bernstein, Numerical estimates of superthermal electron production by ion acoustic waves in the transition region, *J. Geophys. Res.*, 70, 21, 1965.

Freeman, J. W., Jr., The morphology of the electron distribution in the outer radiation zone and near the magnetospheric boundary as ob-served by Explorer 12, *J. Geophys. Res.*, 69, 1691, 1964.

Fried, B. D. and S. D. Conte, *The Plasma Dispersion Function*, Academic Press, New York, 1961.

Fried, B. D. and R. W. Gould, Longitudinal ion oscillations in a hot plasma, *Phys. Fluids*, 4, 139, 1961.

Jackson, E. A., Drift instabilities in a maxwellian plasma, Phys. Fluids, 3, 786, 1960.

Penrose, O., Electrostatic instabilities of a uniform non-maxwellian plasma, Phys. Fluids, 3, 258, 1960.

Scarf, F. L., W. Bernstein and R. W. Fredricks, Electron acceleration and plasma instabilities in the transition region, J. Geophys. Res., 70, 9, 1965.

Sellen, J. M., Jr., and H. Shelton, Transient and steady state behavior in cesium ion beams, in Electrostatic Propulsion, pp. 305 - 356, edited by D. B. Langmuir, J. M. Sellen, Jr., and E. Stuhlinger, Academic Press, New York, 1961.

Sonett, C. P. and I. J. Abrams, The distant geomagnetic field. 3. Disorder and shocks in the magnetopause, J. Geophys. Res., 68, 1233, 1963.

Stix, T. H., The Theory of Plasma Waves, Ch. 9, McGraw-Hill Book Co., New York, 1962.

Strong, I. B., J. R. Asbridge, S. J. Bame, H. E. Felthauser and R. A. Olsen, Positive ion angular, spatial and energy distributions as measured near 17 R_e by an electrostatic analyzer (0.3 to 20 keV), Trans. Am. Geophys. Union, 45, 624, 1964.

Strong, I. B., J. R. Asbridge, S. J. Bame, H. E. Felthauser and R. A. Olsen, Solar wind directional distributions in interplanetary space and the transition region, Trans. Am. Geophys. Union, 46, 134, 1965.

Wolfe, J. H. and R. W. Silva, Results of the NASA-Ames Research Center plasma probe on the Interplanetary Monitoring Plasma, <u>Trans. Am. Geophys. Union</u>, <u>45</u>, 604, 1964.

Wolfe, J. H., R. W. Silva and M. Meyers, Preliminary results from the Ames plasma probe: IMP-1 and OGO-1, <u>Trans. Am. Geophys. Union</u>, <u>46</u>, 119, 1965.

PRODUCTION OF SUPERTHERMAL ELECTRONS
BY ELECTROSTATIC PLASMA OSCILLATIONS

by

R. W. Fredricks

TRW Space Technology Laboratories
Redondo Beach, California

June 2, 1965

Abstract

The beam-plasma interaction which has been proposed by Stix is examined both by approximate analysis and by integration of the nonlinear equations of motion which describe the interaction of an individual electron with a monochromatic large amplitude electrostatic plasma wave. The quasi-stochastic model of the large amplitude plasma waves, introduced by Stix, has been used in the calcualtions by programming a random phase function into the argument of the periodic plasma wave function. It is found that electrons are subject to a quasi-cyclotron acceleration which limits generally at a higher energy in the stochastic case than the limit found in the non-stochastic case (a phase-coherent plasma wave). This behavior is interpreted in terms of a limit cycle phenomenon, and the stochastic phase shift appears to push electrons across these limit cycles. It is also found that favored groups of electrons in a 2eV plasma excited by a 5 keV beam in a 2000 gauss field can achieve energies in the range 85 to 170 keV in less than a nanosecond by a single acceleration occurring in one plasma wave coherence length $L_{\parallel}$ as defined by Stix.

I. INTRODUCTION

In a recent paper Stix[1] has proposed a beam-plasma interaction in which overstable electron plasma oscillations produce cyclotron acceleration of electrons to high energies ($\gtrsim$ 100 keV). A similar mechanism employing overstable ion plasma oscillations has been proposed by Fredricks, et al[2] to explain measurements of superthermal electrons ($\gtrsim$ 40 keV) by spacecraft-borne instruments in the region of interaction between the solar wind (expanding solar coronal plasma) and Earth's magnetic field. This cyclotron acceleration process may be responsible for the production of the energetic electrons ($\gtrsim$ 100 keV) produced when beams of moderate energy (5-20 keV) are passed through a warm plasma ($kT_e \simeq$ 2-20eV) confined in a magnetic mirror field ($B_0 \sim$ 2000G)[3,4,5].

The basic mechanism proposed by Stix[1] is a quasi-stochastic cyclotron acceleration of a selected group (in velocity space) of electrons by electric fields $\underset{\sim}{E}(\underset{\sim}{r}, t)$ due to overstable plasma oscillations excited by the double stream instability. The frequency of oscillation of $\underset{\sim}{E}$ is assumed to be nearly the electron cyclotron frequency, and the velocity group of accelerated electrons contains those which "feel" the wave frequency at their local cyclotron frequency as a consequence of the Doppler shift. Since this acceleration process extracts energy from the wave field (cyclotron damping) it is necessary to show from the dispersion relation that the growth rate of the electrostatic field $\underset{\sim}{E}$ can overcome (or at least balance) the decay rate due to cyclotron damping. The mode considered in detail by Stix is one in which $\underset{\sim}{k} \times \underset{\sim}{E} = 0$, $\underset{\sim}{k} \times \underset{\sim}{B}_0 \neq 0$, that is a mode having components $\underset{\sim}{k}(k_\perp, k_\parallel)$ both perpendicular to and parallel to $\underset{\sim}{B}_0$.

The quasi-stochastic feature of this picture[1] arises from the description of the nonlinear growth of the plasma oscillations to large amplitudes. It is assumed that the primary result of the growth of the nonlinear oscillations is a breaking of the plasma waves leading to large-scale decoherence in the phases of the oscillations in various regions of the plasma. As depicted by Stix, large amplitude oscillations appear as "a conglomerate of

regions of oscillation which are individually coherent but mutually incoherent". The scale size of individually coherent regions is described statistically by introducing a correlation length $L_\parallel$ related to the wavenumber $\underline{k}(\omega)$ of the dominant plasma oscillation. The arguments involved are given by Stix[1] (and are not reproduced here) and he concludes $L_\parallel \approx 0.637 \cdot \lambda_\parallel = 0.637(2\pi/k_\parallel)$.

The effect of introducing such a correlation length for phase coherence is to destroy the particle velocity-position correlations which tend to build up with time, leading to trapped particles and a damping of the nonlinear oscillation to produce a small limiting amplitude of the wave. One of the results of the investigation reported in the present paper is the discovery of a magnetic trapping phenomenon which would severly limit the final energy achieved by an electron subjected to the cyclotron acceleration by a completely coherent wave. However, the introduction of a correlation length for phase decoherence is shown to produce an untrapping which allows particles to be accelerated beyond the limiting energy for fully coherent wave fields of equal amplitude.

The primary difference between the analysis in the present paper and that of Stix[1] is the way in which the equations of motion of the electron are treated. Whereas Stix has attempted to treat the essentially nonlinear differential equations analytically, the present investigation is a combination of approximate analysis and analog computer studies of the equations of motion. Another difference is the way the stochastic phase shift of the plasma oscillation is introduced into the problem. Instead of a correlation length, the computer solutions in this paper were obtained by introducing a random amplitude (between $+ \pi$ and $- \pi$) phase shift ψ into the wave $E_o \cos[\underline{k} \cdot \underline{r} - \omega t + \psi(t)]$. $\psi(t)$ is given a temporal period T_{ph}. For a particle drifting at velocity $V_\parallel$ parallel to the magnetic field, this is equivalent to a correlation length $L_\parallel = V_\parallel T_{ph}$. It is found that the basic mechanism is indeed capable of producing superthermal electrons.

II. APPROXIMATE LIMIT CYCLE SOLUTIONS

Consider an electron in a magnetostatic field $\underset{\sim}{B}_o$ in the Z-direction and an electrostatic oscillation of potential

$$\phi = \phi_o \sin(k_\perp x + k_\parallel z - \omega t + \psi)$$

where ψ is a random phase variable $(-\pi \le \psi \le \pi)$ either of correlation length $L_\parallel$ or of period T_{ph}. The equations of motion are

$$\left. \begin{array}{rcl} \ddot{x} - \omega_c \dot{y} &=& (k_\perp e \phi_o / m)\cos(k_\perp x + k_\parallel z - \omega t + \psi) \\ \omega_c \dot{x} + \ddot{y} &=& 0 \\ \ddot{z} &=& (k_\parallel e \phi_o / m)\cos(k_\perp x + k_\parallel z - \omega t + \psi) \end{array} \right\} \quad (1)$$

The analytical techniques for handling nonlinear equations of the sort in Eqs. (1) are quite limited, although moderate success may be anticipated in cases of "small" forcing terms, that is when the modulus of the r.h.s. of (1), $|\underset{\sim}{k}| e \phi_o / m$, is small compared to some inertial quantity such as $\ddot{x}$, $\ddot{y}$, $\ddot{z}$.

One may expect that solutions to (1) could exhibit, under some circumstances, a limit cycle phenomenon[6]. The plausibility of limit cycle solutions can be demonstrated quite easily in the case $k_\parallel = 0$, $\psi = 0$. One can then assume a periodic orbit of the form $x(t) = R\sin(\omega t + \alpha)$, $y(t) = R\cos(\omega t + \alpha)$, $\alpha = $ const., and examine the time-averaged force over one cyclotron period

$$\langle f_\perp \rangle = (k_\perp e \phi_o / 2\pi m)\int_{\theta_o}^{\theta_o + 2\pi} \cos(k_\perp R\sin(\theta + \alpha) - \omega\theta/\omega_c)\, d\theta \quad (2)$$

where $\theta = \omega t$. The integral in (2) is a Bessel function $J_n(k_\perp R)$ if $\omega/\omega_c = n = 0,1,2,3\ldots$. For non-integral $\omega/\omega_c = \nu$, it is a generalized cylinder function[7] $Z_\nu(k_\perp R)$. In either case, it will be a damped oscillatory function of $k_\perp R$, the zeros of which will be points of either stable or unstable equilibrium depending upon the slope of the function J_n or Z_ν in the vicinity of the zero. The points of stable equilibrium where $\langle f_\perp \rangle = 0$ can be limit cycle orbits. Although it has not been shown here that orbits for which (2) is valid are accessible from arbitrary initial conditions on (1),

at least plausibility of limit cycles may be inferred. It will be seen in Section IV.B. below that analog computer solutions to (1) do indeed exhibit a type of limit cycle behavior.

III. PERTURBATION SOLUTIONS

If the amplitude $k_\parallel e\phi_o/m$ of the forcing term in the third member of Eqs. (1) is small in the sense previously described, one may write an approximate expansion[2]

$$k_\parallel z \simeq k_\parallel z_o + k_\parallel V_\parallel t - (k_\parallel^2 e\phi_o/m\omega^2)\cos[k_\perp x + k_\parallel z_o$$
$$- k_\parallel V_\parallel t - \omega t + \psi] + \cdot\cdot \qquad (3)$$

where z_o is the initial value of $z(t)$ and $V_\parallel$ is the initial value of $\dot{z}$. For For $k_\parallel^2 e\phi_o/m\omega^2 \lesssim 0.1$, the oscillatory term in (3) will introduce phase shifts varying between at most ± 3.6 deg. into the r.h.s. of the first member of (1). If one neglects these small oscillations, then Eqs. (1) degenerate into the transverse equations

$$\ddot{x} - \omega_c\dot{y} = (k_\perp e\phi_o/m)\cos(k_\perp x - \beta\omega_c t + \psi)$$
$$\omega_c\dot{x} + \ddot{y} = 0 \qquad (4)$$

where $\beta = (\omega - k_\parallel V_\parallel)/\omega_c$ is a normalized Doppler-shifted frequency. Eqs. (4) are those treated quasi-statistically by Stix[1] to obtain an expression for the transverse energy $W_\perp^{(N)}$ obtained by an electron after N collisions with the stochastically phased electric field. (It will be shown in Section IV.C. below that under appropriate conditions on the parameters β and $f_\perp = k_\perp^2 e\phi_o/m\omega_c^2$, solutions to (4) can be obtained, for electrons drifting through a single correlation length $L_\parallel \gtrsim V_\parallel T_{acc}$ wherein $\psi = $ const., that yield very energetic electrons. That is, there will be electrons in the tail $\left[v = V_\parallel \gg (2kT_e/m)^{1/2}\right]$ of a cool plasma distribution that can absorb energy from the electric field in a time T_{acc} less than or equal to their drift time across a coherently phased cell of dimension $L_\parallel$.)

A very crude estimate of the behavior of (4) has already been made, resulting in Eq (2) for $\langle f_\perp \rangle$. One can also form an energy rate equation from (4), that is

$$\frac{m}{2} \frac{d}{dt}\left[(\dot{x})^2 + (\dot{y})^2 \right] = \frac{dW_\perp}{dt} = e\phi_0 \beta\omega_c \cos(k_\perp x - \beta\omega_c t + \psi) + e\phi_0 \frac{d}{dt}\sin(k_\perp x - \beta\omega_c t + \psi) \tag{5}$$

If one assumes that the motion ensues on orbits of the sort $x(t) = \rho(t)\sin\omega_c t$, $y(t) = \rho(t)\cos\omega_c t$ where $\rho(t)$ changes very little over the interval $2(m-1)\pi \le \omega_c t \le 2m\pi$, m = integer, then to first order the change in $W_\perp$ over one cyclotron period is

$$\Delta W_\perp \simeq 2\pi e\phi_0 \beta\omega_c \cos\psi Z_\beta(k_\perp\langle\rho\rangle) + 0\,(k_\perp\Delta\rho)\,, \tag{6}$$

where $\langle\rho\rangle$ is the mean value of $\rho(t)$ over this interval, $\Delta\rho$ is the change in $\rho(t)$ and it is assumed that $\Delta\rho \ll \langle\rho\rangle$, and $Z_\beta(k_\perp\langle\rho\rangle)$ is the generalized cylinder function defined by the integral in Eq. (2). The limit cycle phenomenon of (2) is again apparent in (6), because of the zeros of Z_β.

Two cases of interest for the purposes of comparison with later analog solutions to (4) are $\beta = 1$ and $\beta = 2$. If one selects $\cos\psi = 1$ then $\Delta W_\perp \propto J_1(k_\perp\langle\rho\rangle)$ or $J_2(k_\perp\langle\rho\rangle)$. Thus, the energy increments on each quasi-cyclotron orbit would appear to grow at first, until a mean radius $\langle\rho_0\rangle$ corresponding to the first maximum of $J_n(k\langle\rho\rangle)$ is reached. Beyond $\langle\rho_0\rangle$ the successive $\Delta W_\perp$ should continually decrease until the limit cycle orbit $\langle\rho\rangle_{max}$, $J_n(k_\perp\langle\rho\rangle_{max}) = 0$ is reached. The trajectory $x(t)$, $y(t)$ on the X-Y plane would appear to be a non-uniform spiral if (6) is valid (see Fig. 5).

Eq. (6) is only qualitatively correct, and the limit cycle location at $k_\perp\langle\rho\rangle_{max}$ such that $J_n(k_\perp\langle\rho\rangle_{max}) = 0$ may be numerically incorrect. (In fact, analog computation shows that this is the case.) A more refined perturbation analysis can be made by introducing solutions of the type

$$x(t) = \langle\rho\rangle_j \sin\omega_c t + \xi_j(t), \quad y(t) = \langle\rho\rangle_j \cos\omega_c t + \eta_j(t)$$

where $\xi_j(t)$, $\eta_j(t) \ll \langle\rho\rangle_j$, and linearizing equations (4) to first order in ξ_j and η_j. The result is

$$\ddot{\xi}_j - \omega_c \dot{\eta}_j - \left\{ (k_\perp^2 e\phi_0/m)\sin(k_\perp \langle \rho_j \rangle \sin\omega_c t - \beta\omega_c t + \psi) \right\}\xi_j =$$

$$= (k_\perp e\phi_0/m)\cos(k_\perp \langle \rho_j \rangle \sin\omega_c t - \beta\omega_c t + \psi)$$

$$\omega_c \dot{\xi}_j + \ddot{\eta}_j = 0$$

which are valid over $t_j \leq t < t_j + 2\pi/\omega_c$, and $\langle \rho \rangle_j$ is the mean gyroradius during this time interval. If the second of these equations is integrated for initial conditions $\xi_j = 0$, $\dot{\eta}_j = 0$ at $t = t_j$, and we let $\psi = 0$, then a combination of the result with the first equation yields

$$\ddot{\xi}_j + \left\{ \omega_c^2 - (k_\perp^2 e\phi_0/m)\sin(k_\perp \langle \rho \rangle_j \sin\omega_c t - \beta\omega_c t) \right\}\xi_j$$

$$= (k_\perp e\phi_0/m)\cos(k_\perp \langle \rho \rangle_j \sin\omega_c t - \beta\omega_c t) \qquad (7)$$

This equation is approximately valid only up to time $t = t_j + 2\pi/\omega_c$, where $\langle \rho \rangle_j$ must be adjusted to a new value $\langle \rho \rangle_{j+1}$.

Eqs. (7) is an inhomogeneous Hill's equation of the form

$$\ddot{\varphi} + [a - 2qf(t)]\varphi(t) = g(t) \qquad (8)$$

where the functions $f(t)$ and $g(t)$ are expansible into Fourier series on the interval T. The procedural details of solving an equation such as (8) involve infinite determinants, the elements of which are functions of the Fourier expansion coefficients, and can be found for instance in McLachlan[8]. These intricate calculations will not be performed here, since the nonlinear equations (4) have been solved on an analog computer. The equation (7) has been introduced only to demonstrate that the crude result (6) could be further refined if necessary, and the location of the limit cycle given by (6) may well disagree with that found by solving a chain of equations such as (7) where $\langle \rho \rangle_j$ is readjusted after each cyclotron period.

IV. ANALOG COMPUTER RESULTS

A. Stochastic Phase Shifts

For the purposes of analog computation, it is convenient to cast Eqs. (1) into a dimensionless form. One can define the dimensionless variables

and parameters $\xi = k_\perp x$, $\eta = k_\perp y$, $\zeta = k_\parallel z_1$, $z_1 = z + V_\parallel t$, $\tau = \omega_c t$, $\beta = (\omega - k_\parallel V_\parallel)/\omega_c$, $f_{\perp,\parallel} = k_{\perp,\parallel}^2 \, e\phi_0/m\omega_c^2$. Then the equations of motion become in this representation

$$\left. \begin{array}{rcl} \ddot{\xi} - \ddot{\eta} & = & f_\perp \cos(\xi + \eta - \beta\tau + \psi) \\[2mm] \ddot{\xi} + \ddot{\eta} & = & 0 \\[2mm] \ddot{\zeta} & = & f_\parallel \cos(\xi + \eta - \beta\tau + \psi) \end{array} \right\} \quad (\dot{\phi} \to d\phi/d\tau) \qquad (9)$$

The phase function ψ is considered a function of τ, such that it will represent a random amplitude in the range $-\pi \leq \psi \leq \pi$ over a time interval $\Delta\tau = T_{ph}$.

Equations (1) were programmed on an electronic analog computer for various values of $f_\perp$, $f_\parallel$, β and initial data. The phase function ψ was introduced in various forms, ranging from a time independent constant ($\psi = 0$, the case discussed in Section IV.C. below), through a series of pulse periods T_{ph}, to a broadband gaussian noise signal. The dimensionless time intervals over which solutions to (9) were obtained were $0 \leq \tau \leq 1000$, corresponding to some 160 cyclotron periods.

The dimensionless transverse velocity

$$w_\perp = \left\{ (\dot{\xi})^2 + (\dot{\eta})^2 \right\}^{1/2} , \qquad (10)$$

is related to the transverse energy in the following way:

$$W_\perp = \frac{1}{2} m v_\perp^2 = \frac{w_\perp^2}{2f_\perp} (e\phi_0) . \qquad (11)$$

To determine the effect of the random phase shift $\psi(\tau)$ on the energy $W_\perp$ achieved in the time $\tau = 1000$, values $f_\perp = f_\parallel = 1.0$ and $\beta = 1.75$ were selected, and the repetition period T_{ph} was varied. The results of this computation are shown in the bar graph of Fig. 1. The horizontal line at $w_\perp(\text{max}) = 1.8$ shows the maximum velocity reached in the case $\psi(\tau) = 0$ ($T_{ph} \to \infty$) which represents a fully coherent wave. The bar shown at $T_{ph} = 0$ is the result obtained by using a wide band (0 - 100 kc) gaussian noise source to represent $\psi(\tau)$.

The effect of fixing the repetition period of the random phase function at a value T_{ph} = 2.0 and varying the normalized Doppler shifted frequency β is shown in Fig. 2. One can see that over the time period used, the acceleration is rather broad banded with respect to β, at least for the values $f_\perp = f_{||}$ = 1.0. However, this is a case in which the force parameters are "large" in the sense of Sections II and III; in these large force cases, any "resonance" one might expect as a function of β is distorted by nonlinear effects. On the other hand, when $f_\perp$ and $f_{||}$ become small in the sense of Sections II and III, as in Section IV. C. below, the resonance conditions β = n = 1,2 seem to hold approximately, and the broad bandedness inferred from the large force case in Fig. 2 cannot be extrapolated to the small force cases. (This broad or narrow banded behavior of the acceleration process clearly is of importance in assessing the merits of the proposed mechanism for producing energetic electrons. If the forces are large enough to produce a broadband acceleration, large velocity groups of plasma electrons will absorb energy from the plasma wave leading to severe damping effects on the electric field oscillations. This point will be more fully discussed later.)

The transverse energy relation (11) suggested a study of solutions as a function of $f_\perp$, in the hope that the ratio $w_\perp^2(\max)/2f_\perp$ would increase with decreasing $f_\perp$. Also, since $f_{||}$ does not appear explicitly in (11), but is implicit in $w_\perp(\max)$, the effect of varying $f_{||}$ was studied. Table 1 is a list of results $w_\perp(\max)$ obtained by integrating Eqs. (9) from τ = 0 to τ = 1000, for the case β = 1.75. The noteworthy features of these results are: (1) for very large $f_{||}$ the value of $w_\perp(\max)$ is obviously reduced if $f_{||} \gg f_\perp$; (2) solutions for small values of $f_\perp$ and $f_{||}$ yield more favorable ratios (higher $W_\perp$) $w_\perp^2(\max)/2f_\perp$.

As another example of the effect of stochastic phase shift in (9) on the value $w_\perp(\max)$, twenty-six successive integrations of (9) from τ = 0 to τ = 100 were performed, using $f_\perp$ = 5.0, $f_{||}$ = 6.5, β = 1.0, T_{ph} = 2.0. The resulting values $w_\perp$ at τ = 100 for each computer integration are shown in

Fig. 3 as a scatter diagram. The arithmetic average $\bar{w}_\perp = 7.9$ is shown as the horizontal line, and the variance $\Delta w_\perp = \pm \left(\Sigma (w_\perp - \bar{w}_\perp)^2 / N \right)^{1/2}$ is shown as the error flag.

B. Limit Cycles

With reference to Fig. 1, it can be seen that the value $w_\perp$(max) reached by an electron tends to be smaller in the case of a coherent wave ($\psi(\tau) = 0$, the horizontal dashed line in Fig. 1) than that reached for a random phase shift $\psi(\tau) \neq 0$. The conclusion reached by study of the bar graph is that the stochastic phase shift produces forces (or impulses) capable of "kicking" the electron across the limit cycle orbits crudely predicted by Eq. (6). There are probabilities, of course, that the impulses produced by abrupt phase shifts are either decelarative or accelerative. The computer results shown in Fig. 1 indicate, however, that there is a net preference for acceleration. (Unfortunately no growth time studies were made for the computer integrations shown in Fig. 1 because the amount of computer time to furnish adequate statistics would have been prohibitive.)

It seems plausible that there exists a (non-relativistic) practical limit to the transverse energy acquired by an electron under the conditions described by Eqs. (9), since the cylinder function $Z_\beta(k \langle \rho \rangle)$ exhibits damped oscillations as $k_\perp \langle \rho \rangle$ increases. Thus it is reasonable that an orbit (near one of the zeros of Z_β) will be reached where the stochastic pulses due to phase shifting become too weak to energize the electron further. (Perhaps another way to state this is that the growth rates of solutions to Eq. (7) become vanishingly small on these mean orbits.)

Two cases were studied by computer integration in order to empirically establish this sort of limiting behavior. In the first case, the values $f_\perp = f_{\parallel} = 1.0$, $\beta = 1.75$, $T_{ph} = 2.0$ were used in Eqs. (9). The integration proceeded from null initial data at $\tau = 0$ to a final value $w_\perp$(max) = 6.25 at $\tau \leq 1000$. Initial conditions lying outside the limiting orbit $w_\perp = 6.25$ were then selected. These conditions were $\xi(0) = 6.5$, $\dot{\eta}(0) = 1.0$, $\dot{\xi}(0) = \eta(0) = 0$. The solution to (9) was then begun, and at early times in the

integration ($\tau \ll 1000$) a few orbits corresponding to $w_\perp \sim 7.2$ were observed, but for most of the period $0 \leq \tau \leq 1000$ the solution remained in the vicinity of $w_\perp \sim 6.25$.

As a check, a second case in which $f_\perp = 1.0$, $f_{||} = 0.1$, $\beta = 1.75$, $T_{ph} = 2.0$ was studied. For zero initial conditions the value $w_\perp$ (max) = 7.5 was achieved by integration over $0 \leq \tau \leq 1000$. The initial data were then changed to $\dot{\xi}(0) = 10.0$, $\dot{\eta}(0) = 1.0$, $\xi(0) = \eta(0) = 0$, and integration of (9) begun. The solution decayed steadily into the region near $w_\perp = 7.5$ and remained there for most of the integration period $0 \leq \tau \leq 1000$. These two analog integrations of (9) therefore lend strong empirical support to the existence of the practical limit cycle for the acceleration process.

A rather graphical illustration of the existence of several limit cycles interior to the practical limit cycle, and of the capability of the stochastic phase function $\psi(\tau)$ to force electrons across such limit cycles was found in the solution to (9) for the values $f_\perp = 5.0$, $f_{||} = 0$, $\beta = 1.0$. The initial data were $\xi(0) = \eta(0) = 0$, $\dot{\xi}(0) = \dot{\eta}(0) = 0.1$. In this case, the crude analysis [Eq. (6)] yields

$$\Delta W_\perp \simeq 2\pi e \phi_0 \beta \omega_c \cos\psi \; J_1(k_\perp \langle \rho \rangle)$$

which vanishes[7] for $k_\perp \langle \rho \rangle = \underline{3.83}$, 7.02, $\underline{10.17}$, 13.32, $\underline{16.47}$, ... (The roots of J_1 given in italics are those for stable equilibrium.) One can show that $k_\perp \langle \rho \rangle \simeq w_\perp$ since

$$k_\perp \langle \rho \rangle = k_\perp \omega_c \langle \rho \rangle / \omega_c \simeq k_\perp v_\perp / \omega_c = d\left[(k_\perp x)^2 + (k_\perp y)^2 \right]^{1/2} / d(\omega_c t) = w_\perp$$

Two phase functions were used: $\psi(\tau) = 0$, and $|\psi(\tau)| \leq \pi$ with $T_{ph} = 2.0$. The solutions $\dot{\xi}(\tau)$ and $\dot{\eta}(\tau)$ were plotted by an X-Y recorder for $0 \leq \tau \leq 1000$. The coherently phased wave ($\psi = 0$) produced a limiting transverse velocity $w_\perp$ (max) $\simeq 7.2$, corresponding roughly to the second zero of J_1. The solution for the case of phase decoherence ($\psi \neq 0$) on the other hand produced a value $w_\perp$ (max) $\simeq 15.5$, that is somewhere between the fourth and fifth zeros of J_1. Furthermore, dark rings indicated unusually high densities of orbits in the vicinity of $w_\perp \sim 7$, 10 and 13, i.e. near the zeros of J_1. The nature of this

X-Y plot of $w_\perp(\tau)$ is shown in Fig. 4. The lack of a ring near $w_\perp \sim 3.8$ is probably due to the fact that $f_\perp = 5.0$ represents a rather "large" forcing term in the sense of Sections II and III. These results tend to confirm empirically the concept that limit cycles exist, forming "magnetic traps" analogous to the electrostatic trapping phenomenon, and that stochastic phase shifts aid in allowing particles to become untrapped from orbits of lower transverse energy and proceed to orbits of higher energy until some practical limit is reached.

C. Coherent Acceleration and "Resonance"

The case of coherent acceleration was studied for two small force amplitudes, $f_\perp = f_{||} = 0.1$ and 0.05. The normalized frequencies $\beta = (\omega - V_{||}k_{||})/\omega_c = \pm 1$ and ± 2 were found to be "resonant" in the sense that they produced rapid growth of the perpendicular velocity $w_\perp(\tau)$ to its maximum value, while other values of β did not produce rapid growth. The solution $w_\perp(\tau) = \left\{(\dot\xi)^2 + (\dot\eta)^2\right\}^{1/2}$ to Eqs. (9), as displayed on an X-Y plotter for the case $f_\perp = f_{||} = 0.1$, $\beta = 1.0$, is shown in Fig. 5. This trajectory has the non-uniform spiral-like feature discussed in Section III. Each successive loop of the spiral developed over approximately one cyclotron period, that is in $\Delta t \simeq 2\pi/\omega_c$. The trajectory of $w_\perp(\tau)$ for the other cases of interest, namely $f_\perp = f_{||} = 0.1$, $|\beta| = 2.0$ and $f_\perp = f_{||} = 0.05$, $|\beta| = 1.0$, 2.0 are similar in appearance.

From X-Y plots such as Fig. 5, growth curves of $w_\perp(\tau)$ vs τ were computed, and are shown in Figs. 6 and 7. The growth properties were found to be very sensitive to the choice of initial conditions. As an example, immediate growth was obtained only for initial velocity conditions $\underline{w}_\perp(0)$ nearly tangent to the spiral-like trajectory (Fig. 5). Initial conditions violating the near-tangency conditions produced initially decaying solutions $w_\perp(\tau)$ which remained near $w_\perp(\tau) = 0$ for periods long compared to the growth times shown in Figs. 6 and 7. Furthermore, it was determined that even for near-tangent $\underline{w}_\perp(0)$, initial values $w_\perp(0) \lesssim 0.4$ lead to very slowly growing solutions which took (typically) some hundreds of cyclotron periods to

attain values $w_\perp \gtrsim 0.6$. Because of these severe restrictions on initial conditions to obtain rapid growth, it appears to be an empirically established result that only a small and select group of an initial velocity distribution $f(\underset{\sim}{v}_\perp)$ can be "resonantly" accelerated in a given cell of length $L_{\parallel} = V_{\parallel} \, t_{acc}$. In this sense it seems plausible that only small wave damping may result from the production of energetic electrons by this process.

The growth curves for $\beta = 0.9$, 1.1, 1.9, 2.0, 2.1 and 3.0 are shown in Figs. 6 and 7 to illustrate the sharpness of the resonance. Since the computer solutions were allowed to develop only up to $\tau = 50$, the maxima in these cases were not achieved. However, it appears that such a maximum would have occurred only after some hundreds of cyclotron periods.

In Table II we list the maximum transverse energy $W_\perp(max)$ and the acceleration time t_{acc} in units of the peak wave potential $e\phi_0$ and cyclotron period $T_c = 2\pi/\omega_c$ respectively, for the cases $|\underset{\sim}{f}| = 0.1 \sqrt{2}$, 0.05 $\sqrt{2}$ and $\beta = \pm 1, \pm 2$. These values can be computed by inspection of the growth curves in Figs. 6 and 7 and the use of Eq. (11).

V. NUMERICAL EXAMPLES

To illustrate the application of the theoretical results just obtained, they will be used to estimate the accelerations of electrons under conditions of beam-plasma interaction similar to those investigated numerically by Stix[1]. For example, consider with Stix a V_b = 5 kV beam interacting with a plasma of temperature $kT_e \sim 2$ eV, immersed in a magnetic field $B_o \sim 2000G$. Then $\omega_c = 3.5 \times 10^{10} \, sec^{-1}$. The only difference from the parameters employed by Stix is that he uses $k_\perp/k_{\parallel} \sim 0.76$ while $k_\perp/k_{\parallel} = 1.0$ is used here.

If one follows the argument presented by Stix[1] concerning the limiting amplitude $e\phi_o \sim 0.35 \, eV_b = 1770$ eV, then the wave numbers for the cases $f_\perp = 0.1$, 0.05 become

$$\frac{2\pi}{\lambda_\perp} = k_\perp = (f_\perp m\omega_c^2/e\phi)^{1/2} = 6.18 cm^{-1}, \ \lambda_\perp \sim 0.99 \text{ cm for } f_\perp = 0.1$$
$$= 4.38 cm^{-1}, \ \lambda_\perp \sim 0.70 \text{ cm for } f_\perp = 0.05$$

The wavelengths are on the order of those used by Stix. By use of Table 2 one computes the final energies for $f_\perp = 0.05$, $\beta = \pm 1$, ± 2

$$W_\parallel (\text{max}) = 230 \text{ keV, } \beta = \pm 2$$
$$W_\perp (\text{max}) = 170 \text{ keV, } \beta = \pm 1$$
$$\left. \right\} \quad t_{\text{acc}} \simeq 43/\omega_c = 1.23 \times 10^{-9} \text{ sec}$$

while for $f_\perp = 0.1$,

$$W_\perp (\text{max}) = 115 \text{ keV, } \beta = \pm 2$$
$$W_\perp (\text{max}) = 85 \text{ keV, } \beta = \pm 1$$
$$\left. \right\} \quad t_{\text{acc}} \simeq 24/\omega_c = 0.685 \times 10^{-9} \text{ sec}$$

The resonance conditions $\beta = \pm 1$, ± 2 can be used to estimate the velocity groups of electrons subject to this acceleration. Since the coherent accelerations computed in Section IV. C. require that the acceleration occur within one drift time across a coherence length $L_\parallel \simeq 0.637 \lambda_\parallel (= 0.637 \lambda_\perp)$, then the resonance conditions give

$$V_\parallel = \frac{\omega \pm \beta \omega_c}{k_\parallel}$$

and

$$L_\parallel \gtrsim V_\parallel t_{\text{acc}}$$

Since the condition for the plasma overstability according to Stix[1] requires $\omega \simeq 1.063 \omega_c$, then it is easy to show that only the condition $\beta = + 1$, $f_\perp = 0.1$ and 0.05 will yield velocities $V_\parallel$ which satisfy the condition $L_\parallel \gtrsim V_\parallel t_{\text{acc}}$. The other conditions $\beta = -1$ and $\beta = \pm 2$ yield velocities $V_\parallel$ such that $L_\parallel \ll V t_{\text{acc}}$. One obtains

$$V_\parallel = \begin{cases} 3.57 \times 10^8 \text{cm/sec, } \beta = 1, \ f_\perp = 0.1 \\ 5.03 \times 10^8 \text{cm/sec, } \beta = 1, \ f_\perp = 0.05 \end{cases}$$

$$V_\parallel t_{\text{acc}} = \begin{cases} 0.439 \text{ cm, } \beta = 1, \ f_\perp = 0.1 \ (L_\parallel = 0.631 \text{ cm}) \\ 0.345 \text{ cm, } \beta = 1, \ f_\perp = 0.05 \ (L_\parallel = 0.446 \text{ cm}) \end{cases}$$

The conditions $f_\perp = 0.1$, 0.05 and $\beta = +1$ therefore can produce 170 keV and 85 keV electrons by acting on groups of electrons in the 2 eV plasma with narrow velocity bands centered about $V_{\parallel} = 3.57 \times 10^8$ cm/sec and 5.03×10^8 cm/sec. To determine how many electrons are subject to this acceleration, consider a 2 eV maxwellian distribution. The mean thermal speed $a = (2kTe/m)^{1/2}$ $= 8.4 \times 10^7$ cm/sec. Hence one has for the value of the Gaussian either

$$e^{-V_{\parallel}^2/a^2} \simeq e^{-18} = 1.54 \times 10^{-8}, \quad \beta = 1, \quad f_\perp = 0.1, \quad W_\perp(\text{max}) = 85 \text{ keV}$$

or

$$e^{-V_{\parallel}^2/a^2} \simeq e^{-36} = 2.37 \times 10^{-16}, \quad \beta = 1, \quad f_\perp = 0.05 \quad W_\perp(\text{max}) = 170 \text{ keV}$$

and it can be seen that very few electrons will experience the resonant acceleration.

VI. SUMMARY DISCUSSION

A basic assumption made by Stix[1] that beam-plasma interactions in a magnetic field can produce large amplitude plasma oscillations with electric fields which are capable of producing very energetic electrons has been explored by integrating the equations of motion of an electron in such fields on an analog computer. Some crude results of analysis of the nonlinear equations of motion have been compared to the computer results, and qualitative agreement obtained.

The occurrence of limit cycle phenomena in the transverse acceleration has been discussed on the basis of a time average treatment of the equations of motion, and apparently verified empirically by the analog computer solutions. The role of Stix's[1] phase coherence correlation length in untrapping electrons from limit cycle orbits has been investigated by computer solutions using random phase functions in the argument of the periodic electrostatic wave.

It has been found that when the dimensionless force parameter $f = k^2 e\phi_0/m\omega_c^2$ is large enough, the transverse energy achieved is limited to

small multiples of $e\phi_0$, and the acceleration is broadbanded in the Doppler-shifted frequency $\omega - k_{||}V_{||}$. However, as f becomes small the acceleration becomes "resonant", the conditions being $\omega - k_{||}V_{||} = \pm \beta\omega_c$, $\beta = 1,2$. The maximum transverse energy at resonance can then be one to two orders of magnitude greater than $e\phi_0$.

The numerical example of a 5 -kV beam interacting with a 2eV plasma in a 2000 G field, treated by Stix[1] on the basis of his quasi-stochastic acceleration mechanism, has been investigated on the basis of the analog computer results of the present paper. It is found that under conditions compatible with the numerical values used by Stix, 85 to 170 keV electrons can be produced in times on the order of 0.7 to 1.2 nanoseconds by a coherent wave acceleration which occurs in one correlation length $L_{||}$ as defined by Stix. The fractional number density of electrons subjected to such acceleration is estimated to be small compared to the total number density, so that cyclotron damping effects should be negligible.

<div align="center">

ACKNOWLEDGEMENTS

</div>

TABLE I. Maximum Transverse Velocities for Stochastic Acceleration.

$\beta = 1.75$, $\dot{\xi}(0) = \dot{\eta}(0) = 1$, $\xi(0) = \eta(0) = 0$, $T_{ph} = 2.0$, $0 \leq \omega_c t \leq 1000$

$f_\perp$	100	10	1	1	0.8	0.6	0.4	0.2	0.1	1.0
$f_\parallel$	100	10	10	0.1	0.8	0.6	0.4	0.2	0.1	0
$w_\perp(\text{max})$	37.0	12.5	5.5	7.5	4.3	3.8	3.0	4.0	3.2	9.0
$w_\perp^2(\text{max})/f_\perp$	6.85	7.80	15.13	28.13	14.5	20.0	28.1	200	51.2	40.5

TABLE II. Transverse Energies and Acceleration Times for Coherent Acceleration.

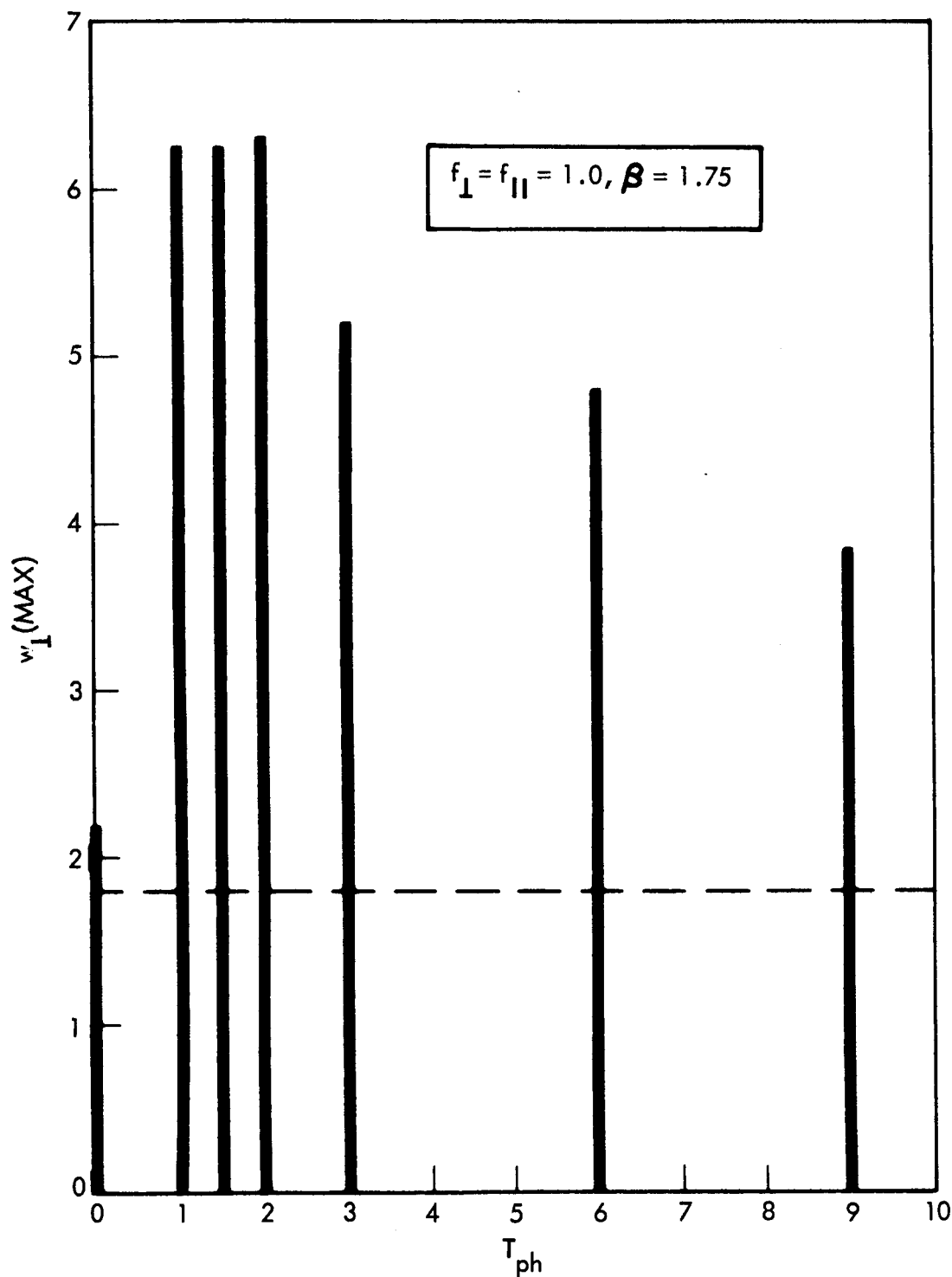| $\pm\beta$	1	1	2	2
$f_\perp$	0.05	0.10	0.05	0.10
$w_\perp(\text{max})$	96 $e\phi_o$	48 $e\phi_o$	130 $e\phi_o$	65 $e\phi_o$
t_{acc}	$43/\omega_c$	$24/\omega_c$	$43/\omega_c$	$24/\omega_c$

Figure 1. Bar graph showing the limiting amplitudes of w_1 reached in the time interval $0 \leq \tau \leq 1000$ as a function of the period T_{ph} of the stochastic phase function $\psi(\tau)$. The bar at $T_{ph} = 0$ is the limiting amplitude reached when $\psi(\tau)$ was generated by a broad band gaussian noise source. The horizontal dashed line is the amplitude reached in the non-stochastic case $\psi(\tau) = 0$.
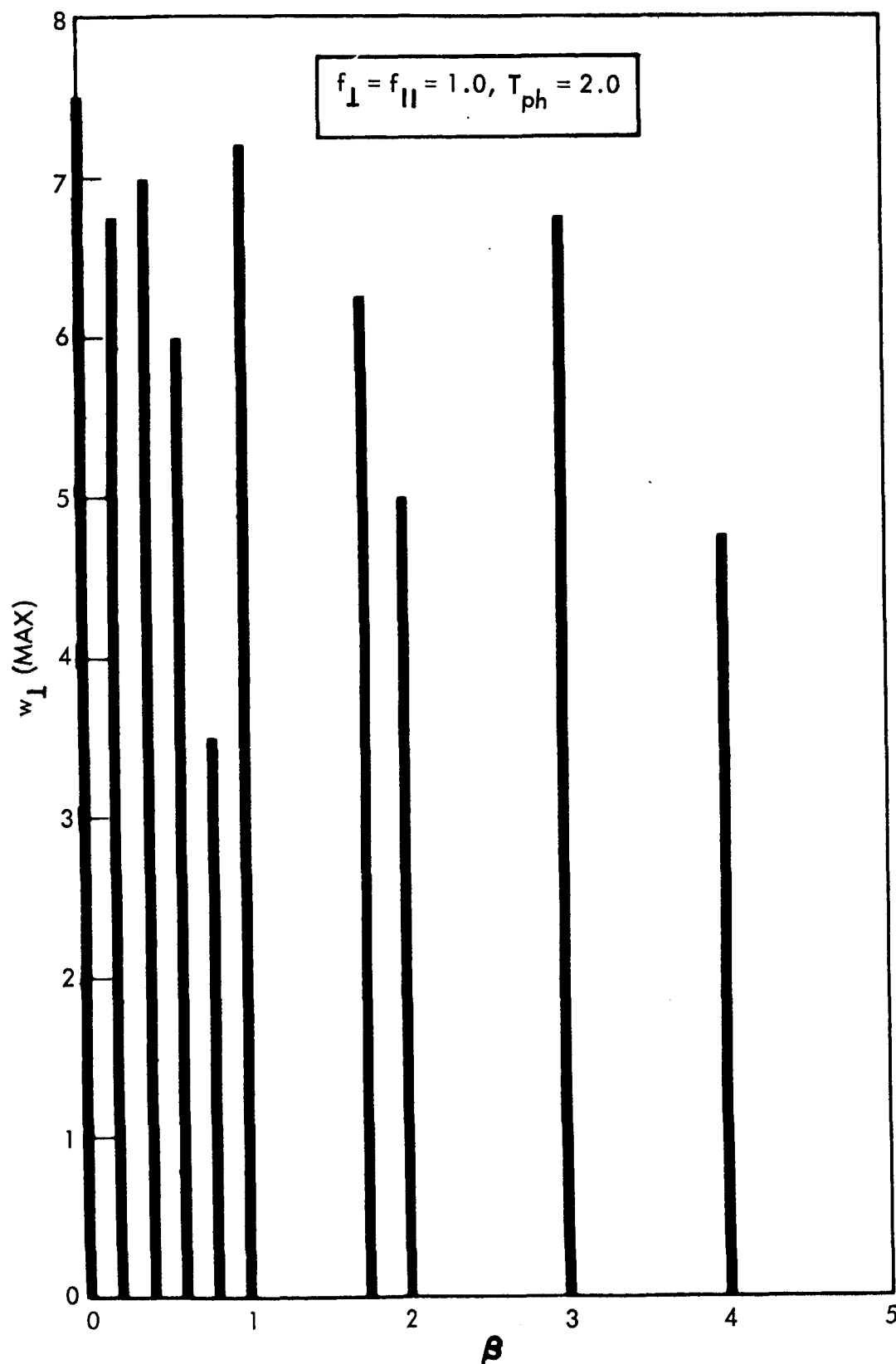
Figure 2. Bar graph showing the limiting amplitudes of $w_\perp$ reached in the time interval $0 \le \tau \le 1000$ as a function of the dimensionless frequency parameter β for a fixed period $T_{ph} = 2$ of the stochastic phase function $\psi(\tau)$.
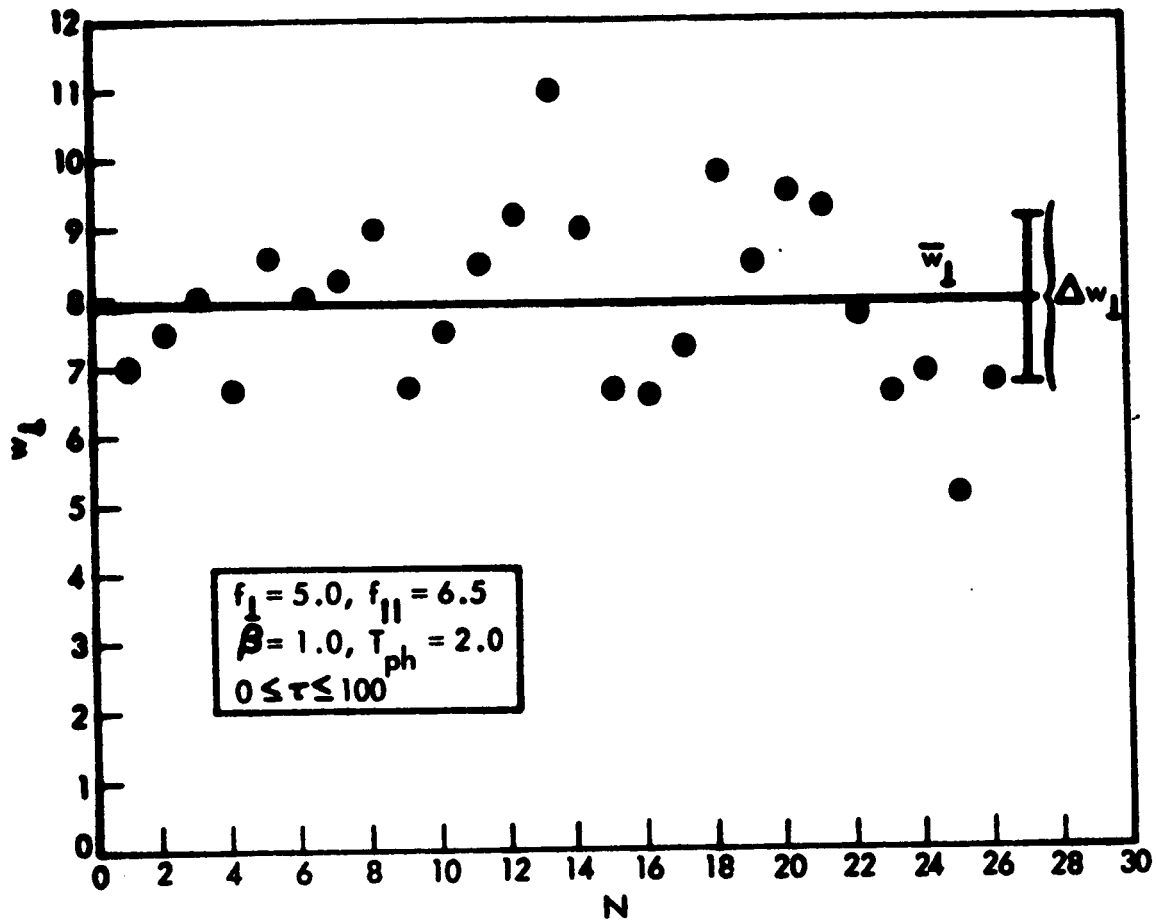
Figure 3. Scatter diagram of the maximum value of $v_\perp$ reached in the time period $0 \leq \tau \leq 100$ for the case $f_\perp = 5.0$, $f_{\parallel} = 6.5$, $\beta = 1.0$ and $T_{ph} = 2.0$. The arithmetic mean $\bar{v}_\perp$ is the solid horizontal line, and the variance $\Delta v_\perp = \pm \left\{ \Sigma \left(v_{\perp_J} - \bar{v}_\perp \right)^2 / N \right\}^{1/2}$, $J = 1,2..N$. is shown as an error flag. $N = 26$ integrations were performed.
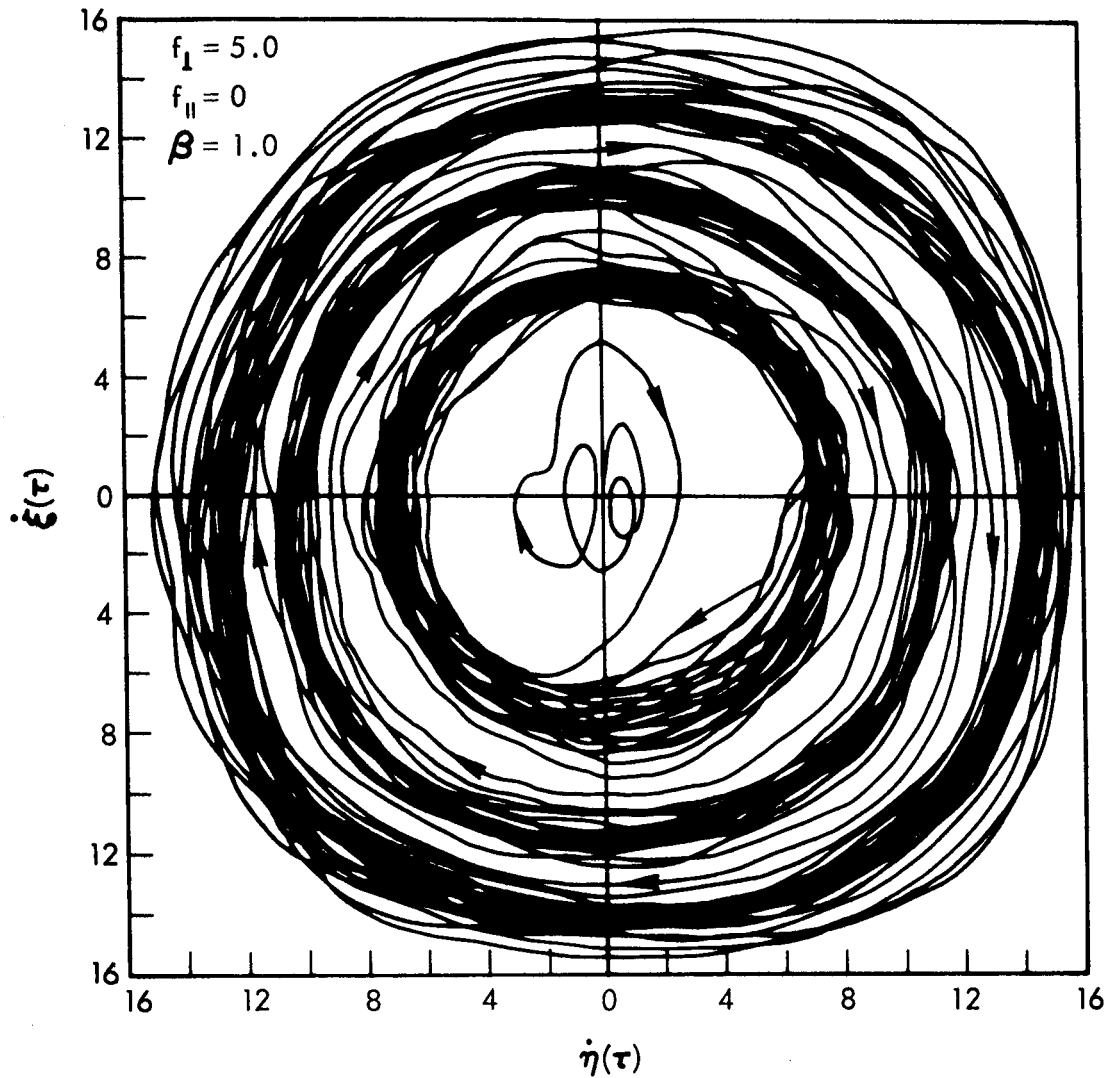
Figure 4. Trajectory of $w_\perp(\tau)$ in the case $f_\perp = 5.0$, $f_{||} = 0.0$, $\beta = 1.0$.
Note the higher density of trajectories near the values
$w_\perp = 7$, 10, 13. The zeros of $J_1(w_\perp)$ are $w_\perp = 3.83$, 7.02, 10.17,
13.32, $16.47...$. The integration period was $0 \leq \tau \leq 1000$ using
a period $T_{ph} = 2.0$ for the random phase function $\psi(\tau)$. The
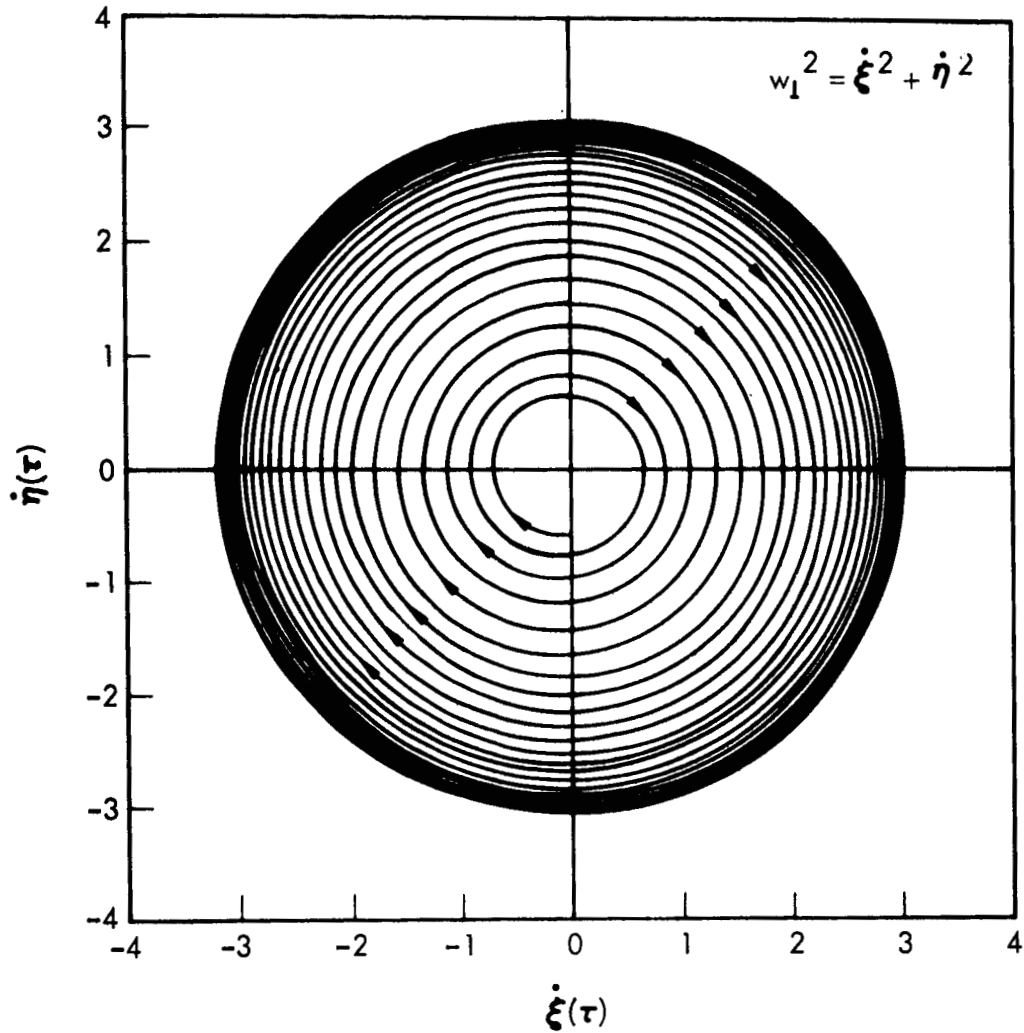limiting value for the coherent wave $\psi(\tau) = 0$ was $w_\perp = 7.2$.

Figure 5. A typical trajectory of $w_\perp(\tau)$ for an electron accelerated under the condition $f_\perp = f_{||} = 0.1$, $\beta = 1.0$. The magnetic field is normal to the plane of the figure. Note the non-uniform spiral, each circuit of which corresponds to nearly $\Delta t = 2\pi/\omega_c$. All "small" force cases (see Section II of text) exhibit such spiral-like trajectories.
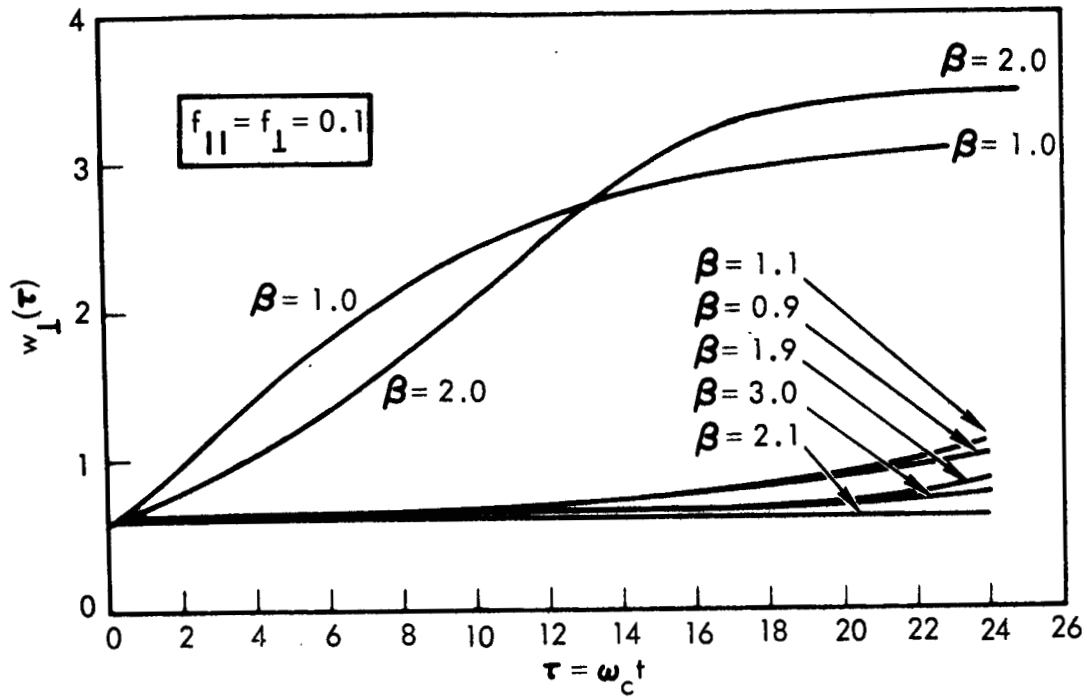
Figure 6. Nonlinear growth curves of normalized transverse velocity
$w_{\perp}(\tau)$ under the conditions $f_{\perp} = f_{\|} = 0.1$, $|\beta| = 0.9$, 1.0, 1.1,
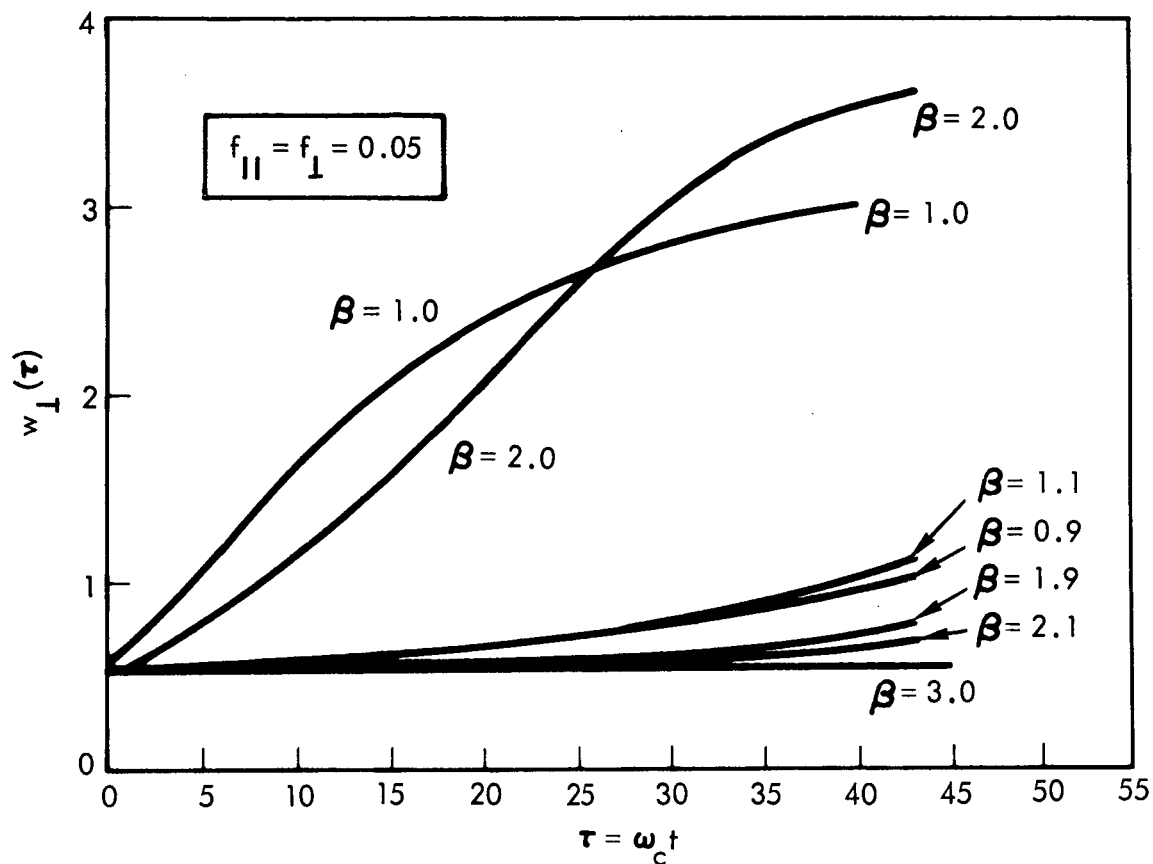1.9, 2.0, 2.1 and 3.0. The cases $\beta = \pm 1.0$, ± 2.0 "resonate".

Figure 7. Nonlinear growth curves of normalized transverse velocity
$w_\perp(\tau)$ for the same values of $|\beta|$ as those in Fig. 6. Here
$f_\perp = f_{||} = 0.05$. Again, the cases $\beta = \pm 1.0$, ± 2.0 "resonate".

References

1. T. H. Stix, Phys. Fluids $\underline{7}$, 1960 (1964).

2. R. W. Fredricks, F. L. Scarf and W. Bernstein, J. Geophys. Res. $\underline{70}$, 21 (1965); F. L. Scarf, W. Bernstein and R. W. Fredricks, J. Geophys. Res. $\underline{70}$, 9 (1965).

3. I. Alexeff, R. V. Neidigh and W. F. Peed, Phys. Rev. $\underline{136}$, A689 (1964).

4. L. D. Smullin and W. D. Getty, Phys. Rev. Letters $\underline{9}$, 3 (1962).

5. I. F. Kharchenko, Ya. B. Fainberg, R. M. Nikolayev, E. A. Kornilov, E. I. Lutsenko, and N. S. Pedenko, Nucl. Fusion Suppl. Pt. 3, 1101 (1962).

6. See, for instance, N. Minorsky, Introduction to Non-Linear Mechanics, Edwards Brothers, Ann Arbor, Mich. (1947).

7. See, for example, E. Jahnke and F. Emde, Tables of Functions, Dover Publications, New York (1945).

8. N. W. McLachlan, Theory and Application of Mathieu Functions, Oxford Univ. Press, London (1947).